UNHINGED ENCODES A VPS51 HOMOLOGUE OF ARABIDOPSIS AND REVEALS A ROLE FOR THE GARP COMPLEX IN LEAF SHAPE AND VEIN PATTERNING

SHANKAR PAHARI
M.Sc. University of Lethbridge, 2008

A Thesis
Submitted to the School of Graduate Studies
of the University of Lethbridge
in Partial Fulfilment of the
Requirements for the Degree

DOCTOR OF PHILOSOPHY

Biological Sciences
University of Lethbridge
LETHBRIDGE, ALBERTA, CANADA

DEDICATION

In loving memory of my father, Jagannath Pahari who passed away during the production of this thesis

ABSTRACT

Asymmetric localization of PIN proteins controls directionality of auxin transport and many aspects of plant development. The *Arabidopsis* mutant, *unhinged-1 (unh-1)*, has defects to leaf veins and other root and shoot phenotypes. I identify *UNH* as the *Arabidopsis* VPS51 homologue, a member of the *Arabidopsis* GARP complex, and show that UNH interacts with VPS52, another member of the complex. I also show that UNH co-localizes with SYP61, a trans Golgi network marker. The GARP complex in yeast and metazoans retrieves vacuolar sorting receptors to the TGN and is important in sorting proteins for lysosomal degradation. PIN1 expression in the margin of *unh-1* leaves is expanded and the *unh* leaf phenotype is suppressed by *pin1* mutation, supporting the idea that the phenotype results from expanded PIN expression. My results suggest that UNH is important to restrict expression of PIN1 within the margin, likely by targeting PIN1 to the lytic vacuole.

ACKNOWLEDGEMENTS

I would like to wholeheartedly thank my supervisor, Dr. Elizabeth Schultz, Associate Professor of Biology, for her consistent guidance, support and encouragement throughout my program. I wish to acknowledge my supervisory committee members, Dr. Roy Golsteyn, Associate Professor of Biology and Dr. Marc Roussel, Professor of Chemistry, for their valuable comments, suggestions and insightful discussions.

I am thankful to the members of Schultz's lab, Ryan, Mike, Hongwei, Neema, Jessica, Chen, Jordan, Emily and Vanessa for their cooperation, help and support in many ways. I would also like to thank Doug Bray, Biological Science, for his technical help in confocal microscopy. I am thankful to the Helper Hall family for all the help and assistance I got during my research.

I am grateful to the University of Lethbridge, the Graduate Studies and Biological Sciences family for giving me an opportunity to work as a graduate student and for the financial support.

My sincere gratitude goes to my family for their persistent love, care and patience. It would not have been possible without their contributions. I wish my father were with us to celebrate this accomplishment.

TABLE OF CONTENTS

LIST OF TABLES

LIST OF FIGURES

LIST OF ABBREVIATIONS

Gene and Protein annotation

UNHINGED – wild type gene is capitalized and italicized

unhinged – mutant gene is italicized

UNHINGED – protein is capitalized

……..

ABC = ATP Binding Cassette

AGL4 = AGAMOUS LIKE4

ANG2 = ANOTHER NEW GENE2

AP2 = Apetala2

ARF = Auxin Response Factor

Arf = ADP- Ribosylation Factor

AS1 = ASYMMETRIC LEAF1

ATHB8 = HOMEOBOX GENE 8

AUX1/LAX = Auxin Resistant1/Like Aux1

BAC = Bacterial Artificial Chromosome

BFA = Brefeldin A

chmp1a= charged multivesicular body protein/chromatin modifying protein1a

CIMPR = Cation Independent Mannose-6 Phosphate receptor

COP = Cytoplasmic Coat Protein

CPY = carboxypeptidaseY

CUC2 = CUPSHAPED COTYLEDON2

DAG = Days After Germination

DSL1= Dependence on SLy1-20

EE = Early Endosomes

eir = ethylene insensitive root

EMS = Ethyl methane sulfonate

ESCRT = Endosomal Sorting Complex Required for Transport

FKD1 = FORKED1

GAL4 = GALactose metabolism 4

GAP = GTPase-activating protein

GARP =Golgi Associated Retrograde Protein

GEF = GTP exchange factor

GFP = Green Fluorescent Protein

GUS = β-GLUCORONIDASE

hit1-1= heat-intolerant1-1

HOPS = homotypic vacuole fusion and vacuole protein sorting

IAA = indole-3-acetic acid

LacZ = B-GALACTOSIDASE.

LE = Late Endosomes

Ler = Landsberg erecta

LLD = Lower Loop Domain

max = more axillary branching

MDR = Multi-Drug Resistant

MP = MONOPTEROS

MVB = Multivesicular Bodies

NOA = naphthoxyacetic acid

pBI = pBluescript

PC = pavement cells

PEDs = PIN1 Expression Domains

PGP = P-Glycoprotein

PID = PINOID

PIN = PIN FORMED

PLT = PLETHORA.

pok = poky pollen tube

PP2A = Protein Phosphatase

PVC = Prevacuolar complex

QC = Quiescent Centre

Ras = Ras related Nuclear

Sar1 = Secretion-Associated Ras1

SAUR = Small Auxin Up RNA

SNAREs = Soluble *N*-ethylamide-sensitive factor Attachment protein Receptors

SNC1 = Suppressor of the Null allele of CAP

SNPs = single nucleotide polymorphisms

SNX = Sorting Nexin

SSLPs = Simple sequence length polymorphisms

SYP = Syntaxin of Plants

TEM = transmission electron microscope

TGN = Trans Golgi Network

TIR = Transport Inhibitor Response

tir1 = Toll/IL-1 receptor/plant disease resistance gene

TLG = T-snare affecting a Late Golgi compartment

TRAPP = Transport Protein Particle

Trp = Tryptophan

ULD = upper loop domain

UNH = UNHINGED

VAM3 = Vacuolar Morphology 3

VPS = Vacuolar Protein Sorting

VSRs = Vacuolar Sorting Receptors

VTI11 = VESICLE TRANSPORT V-SNARE 11

WT = wild type

YFP = yellow Fluorescent Protein

YPT6 = Yeast Protein Two 6

CHAPTER 1: INTRODUCTION

1.1 Auxin - general background

Unlike animals, many of the tissues and organs in plants originate *de novo* during postembryonic development. This gives plants an opportunity to shape the body plan based on environmental and intrinsic signals. Plants have acquired a high capacity for tissue regeneration and a precisely regulated developmental and phenotypic plasticity that they can utilize according to their needs. Common examples include response of plant shoots towards a light source (phototropism) or that of roots towards gravity stimulus (gravitropism). Plant hormones are key signaling molecules by which plants can respond to such changes in environmental and growth signals. Auxin is a plant hormone that has critical roles in many aspects of plant development and will be a focus of this thesis.

The discovery of the phytohormone auxin dates back to the late 19th century. When Darwin and his son francis were doing experiments in phototropism, they saw that the coleoptile tip of canary grass bent towards a source of unidirectional light. The bending did not happen when the tip was removed or covered with aluminum foil (Darwin and Darwin, 1892). They concluded that there was a signal in the tip that, in response to light, moves and causes the unequal growth required for bending. It was later shown that the growth promoting substance in the tip was able to restore growth; hence, it was given the name auxin - in Greek *auxein* means to elongate or grow. The chemical nature of this substance was revealed as being Indole-3-Acetic Acid (IAA). IAA is the predominant auxin in higher plants (Went and Thimann, 1937).

In addition to its role in plant growth and tropism, auxin controls a plethora of other developmental processes including organ initiation and tissue patterning. It was not clear how auxin could account for such a wide spectrum of plant developmental processes until the discovery that a group of auxin transporters are responsible for cell to cell auxin movement (Bennett et al., 1996; Galweiler et al., 1998; Rubery and Sheldrak, 1974). Further, the discovery of auxin-responsive promoters such as Small Auxin Up RNA (SAUR) and DR5 and reporter genes such as β-Glucuronidase (GUS) and Green Fluorescent Protein (GFP) provided researchers a convenient method for studying and visualizing auxin gradients within specific organs and tissues (Friml et al., 2003; Li et al., 1991; Sabatini et al., 1999; Ulmasov et al., 1997).

Auxin transport and differential auxin gradients affect embryonic and post – embryonic development. During embryogenesis, auxin establishes the polarity and division planes of the zygote, causes cell division to form progressive stages of embryogenesis and determines root and shoot initials. Further, auxin contributes to organ initiation (lateral root, root hair and leaf initiation); cell differentiation (cell shape and size, root hair development and vascular cell formation) and environmental response (phototropism and gravitropism) (Benkova et al., 2003; Blilou et al., 2005; Friml, 2003; Friml and Palme, 2002; Sabatini et al., 1999; Vieten et al., 2005). The key to these functions is the differential auxin gradient (Friml, 2003). Defects in the formation of the appropriate auxin gradient at these stages affect the polarity and division of the zygote and initiation of root and shoot organs (Blilou et al., 2005; Vieten et al., 2005).

Temporal and spatial distribution of auxin depends on the combined effects of 1) auxin synthesis, 2) auxin conjugation, 3) auxin degradation and 4) auxin transport. Together these processes maintain the auxin pool at a level optimal for growth and development. These processes are tightly regulated by external and internal growth stimuli at both transcriptional and post-transcriptional levels (Bartel, 1997; Ljung et al., 2001; Ljung et al., 2005; Ljung et al., 2002).

1.1.1 Auxin synthesis, conjugation, hydrolysis and degradation

IAA is the most abundant naturally occurring form of auxin in plants (Went and Thimann, 1937). Although most tissues display some IAA synthesis capacity, IAA is predominantly synthesized in young, developing tissues, such as shoot apical meristem and young leaves (Ljung et al., 2001; Zhao, 2010). Several pathways are involved in auxin biosynthesis, the common precursor being the amino acid Tryptophan (Trp) (Bartel, 1997; Zhao, 2010). Studies in mutants with reduced levels of Trp synthase suggest that tryptophan-independent pathways also exist in plants (Last et al., 1991; Normanly et al., 1993), however less is known about the latter pathways. Most of the auxin exists as either amide conjugates or ester conjugates. Auxin conjugation is important because the conjugates act as a reserve pool for auxin homeostasis and protect auxin against oxidative decay (Cohen and Bandurski, 1982; Tam et al., 2000). Auxin conjugation is a temporary state, which is reversible upon hydrolysis. During developmental processes auxin is hydrolyzed from its conjugated form by specific hydrolases to release the active free auxin (Bartel, 1997; Fluck et al., 2000) which now is able to travel to the site of action. Finally, auxin degradation

occurs *via* oxidative or decarboxylation pathways (Normanly and Bartel, 1999; Ostin et al., 1998).

1.1.2 Auxin transport

Together with auxin synthesis, conjugation and hydrolysis, auxin transport is important in defining the auxin gradients. Since auxin synthesis is restricted to the aerial parts of the plants, especially the young developing leaves, this source is important for rest of the plant and therefore auxin must move from its site of synthesis to the site of action (Ljung et al., 2001). Two major modes of transport occur: 1) long distance transport of auxin (vascular transport) occurs *via* phloem over a long distance (Bandyopadhyay et al., 2007; Ljung et al., 2005; Swarup et al., 2001) and 2) short distance transport occurs by a process called polar auxin transport (Friml and Palme, 2002; Muday and DeLong, 2001). Of these two pathways, cell-to-cell directional polar auxin transport is the major transport pathway whose control defines the major plant developmental events.

1.2 Polar auxin transport

The chemiosmotic model for polar auxin transport established in the 1970s suggested that there are two classes of auxin transporters: one that imports auxin from the extracellular space into the cell, and the other that exports auxin from the cell to the extracellular space (Rubery and Sheldrak, 1974). The process involves chemiosmotically driven cell-to-cell polar transport of auxin such that each cell is involved in the process (Figure 1.1; Lomax et al., 1995). The carrier dependent

involvement of each and every cell along the transport pathway gives an opportunity for a cell to establish rate and directionality of auxin transport.

IAA, a weak organic acid with a dissociation constant of pK = 4.8, exists mostly in anionic form (a 5:1 ratio for IAA^-: IAA) in the slight acidic (pH 5.5) environment of the apoplast. Auxin can enter the cytoplasm, which has a relatively basic (pH 7) environment, by passive diffusion of IAA or carrier dependent anionic uptake of IAA^- (Figure 1.1; Lomax et al., 1995). The latter is important as diffusion of just 20% of total auxin (IAA) is predicted to enter cell by a level insufficient to account for the rate and magnitude of carrier dependent effluxes exhibited in plants (Kramer and Bennett, 2006). This explains the importance of membrane localized carrier proteins (Galweiler et al., 1998; Steinmann et al., 1999; Swarup et al., 2004). In the cytoplasm, IAA dissociates to IAA^- and H^+ which require efflux carriers to exit from the cell (Galweiler et al., 1998; Steinmann et al., 1999; Swarup et al., 2004). The localization and activity of these influx and efflux carriers are crucial to establishing the auxin transport routes required for plant growth (Bennett et al., 1996; Steinmann et al., 1999).

1.2.1 Classes of polar auxin transporters

Proteins that facilitate the influx and efflux during auxin transport have been characterized in *Arabidopsis*. These proteins are grouped into three major classes; 1) Auxin Resistant1/Like AUX1 (AUX1/LAX) influx transporters, 2) P-Glycoprotein (PGP) also called Multi-Drug Resistant (MDR) efflux transporters and 3) Pin-Formed (PIN) family of efflux carriers.

1.2.1.1 AUX1/LAX influx carriers

AUX1/LAX proteins are members of an amino acid/auxin permease family and were identified in a genetic screen for *Arabidopsis* agravitropic mutants that showed resistance to 2,4-Dichlorophenoxyacetic acid (2,4-D) (Bennett et al., 1996). *AUX1* encodes a plasma membrane protein that acts as a proton-driven symporter to facilitate the influx of IAA^- and H^+ simultaneously (Bennett et al., 1996; Swarup et al., 2004). The agravitropic phenotype of the *aux1* mutant can be phenocopied by treating wild-type seedlings with Naphthoxyacetic *Acid* (NOA), an auxin influx inhibitor (Parry et al., 2001) suggesting that auxin influx is important during gravitropic response (Rashotte et al., 2001). When expressed in *Xenopus* oocytes, AUX1 promoted auxin influx indicating that AUX1 is sufficient for auxin influx (Yang et al., 2006).

1.2.1.2 PGP efflux carriers

Efflux of auxin is exclusively carrier mediated, involving the activity of members of the PIN family (Galweiler et al., 1998), and members of the MDR/PGP subfamily of ATP Binding Cassette (ABC) transporters (Muday and DeLong, 2001). The localization of PGP transporters, unlike PIN (see below), is apolar (Petrasek et al., 2006) such that auxin can exit from any face of the cell. This feature of PGP transporters therefore might control the amount of auxin available for PIN transporters and hence provide specificity of PIN mediated auxin efflux (Blakeslee et al., 2007). The role of PGP in auxin transport is exemplified by a mutation in a gene encoding AtPGP19/AtMDR1, an auxin inducible member of the PGP family, which

results in dwarfed seedlings with reduced polar auxin transport (Noh et al., 2001).

1.2.1.3 PIN efflux carriers

PIN proteins belong to a plant-specific family of transmembrane proteins, which show an asymmetric subcellular localization in the plasma membrane and function as auxin efflux transporters (Galweiler et al., 1998). There are 8 members in the family (PIN1-PIN8) identified in *Arabidopsis* and 5 of these (PIN1, PIN2, PIN 3, PIN 4, PIN 7) are shown to be involved in auxin efflux in *Arabidopsis* as well as when expressed in heterologous systems such as tobacco BY-2, human hela and yeast culture cells (Petrasek et al., 2006). First discovered as conferring a pin shaped inflorescence, mutation in *PIN1* results in defects, such as altered phyllotaxis, organogenesis and vascular patterning, similar to defects shown by plants treated with auxin transport inhibitors (Okada et al., 1991; Sieburth, 1999; Mattsson et al., 1999). The phenotypes are subtle in single or double mutants when compared to the phenotype of plants quadruply mutant for PIN1, PIN3, PIN4, PIN7 (Blilou et al., 2005; Vieten et al., 2005).

1.3 PIN localization

1.3.1 PIN localization during embryogenesis

Mutation in *PIN1* affects bilateral symmetry of the embryo. *pin1* mutants show defects to cotyledon positioning, number, growth and separation (Bennett et al., 1995; Okada et al., 1991). Similar to *pin1* mutation, mutations in *MONOPTEROS* (*MP),* a transcriptional activator of PIN, result in defects to embryo axis formation,

cotyledon positioning and separation (Berleth and Jurgens, 1993; Hardtke and Berleth, 1998). Multiple *pin* mutations give a phenotype more severe than a single or double mutant phenotype, a ball-shaped embryo without apical-basal polarity in the most extreme cases (Friml et al., 2003). This indicates a key role for these genes during embryonic development, which is explained by their dynamic changes in subcellular localization in different cell types (Benkova et al., 2003; Blilou et al., 2005; Vieten et al., 2007; Vieten et al., 2005).

During embryogenesis, apical basal polarity is established by the coordinated action of PIN1, PIN4 and PIN7 (Friml et al., 2003; Mayer and Jurgens, 1998). At the very early stage, PIN7 is localized to the apical (upper) face of the suspensor cell allowing the flow of auxin towards the proembryo (Figure 1.2). PIN1 is expressed during the early globular stage and is localized in a non-polar fashion within upper cells of the embryo. Later, during the mid-globular stage, PIN1 becomes basally (in the face towards the base) localized (Friml et al., 2003). Concurrently, PIN7 in the suspensor is also relocated basally. During the early heart stage PIN4 is activated and localized basally such that auxin flows towards the hypophysis. The hypophysis is the uppermost suspensor cell of the embryo that will give rise to root quiescent centre and root cap initials (Friml et al., 2003; Scheres et al., 1994). The combined action of PIN1, PIN4 and PIN7 directs auxin flow towards the base of the embryo defining the activity of the future root. Also, during the early heart stage, PIN1 polarity in the epidermal cells of the proembryo switches and is localized apically defining the auxin concentration required for embryonic leaf (cotyledon) initiation (Friml et al., 2003).

1.3.2 PIN localization during post embryonic development

1.3.2.1 Role of auxin transport in root development

The loss of function *pin* mutants indicate the biological significance of PIN localization during root development; For example, the *ethylene insensitive root* (*eir)/pin2* and *pin3* mutants show altered gravitropic response (Luschnig et al., 1998; Marchant et al., 1999). During postembryonic development of the root, PIN1, PIN 3, PIN4 and PIN7 show basal localization in the root vasculature contributing to auxin maxima of the Quiescent Centre (QC) (Blilou et al., 2005). Auxin concentration at the QC by the coordinated action of these PIN proteins activates the expression of *PLETHORA* (*PLT*). *PLT* encodes a member of AP2 (Apetala 2) family of transcription factors responsible for maintaining the QC activity (Blilou et al., 2005).

PIN2 shows apical localization in the epidermis and basal localization in the cortex (Luschnig et al., 1998; Muller et al., 1998). The apical localization of PIN2 in the epidermis contributes to gravitropic response and its basal localization at the cortex helps bring the epidermal auxin back to the QC again contributing to the auxin maxima of the QC (Figure 1.3). PIN3 is localized symmetrically in the root columella cells directing the auxin flow away from the QC. When the gravitropic stimulus is altered, PIN3 rapidly re-localizes laterally towards one side of the cell so as to establish asymmetric auxin distribution (Friml et al., 2002). Simultaneously, PIN2 at the epidermal cells regulates the differential auxin transport rates required for differential growth between two sides of the root (Chen et al., 1998; Shin et al., 2005).

1.3.2.2 Role of auxin transport in leaf shape and vein patterning

Dynamic PIN1 localization in epidermis and procambial cells in the leaves has implications for leaf development, leaf vein patterning and cell shape.

The leaf vein patterning is important for two main reasons: 1. it provides mechanical support for the plants and 2. it transports water and nutrients. Therefore the interconnection and density of veins have implications from the physiological and ecological perspectives.

Leaf vein patterning in *Arabidopsis* is a progressive and hierarchical process such that new veins form in continuation with the pre-existing veins to form a final, reticulate structure (Berleth and Mattsson, 2000; Berleth et al., 2000; Scarpella et al., 2004; Steynen and Schultz, 2003). A widely accepted model for vein formation is the auxin canalization hypothesis, a self-organizing model. The model states that a positive feedback mechanism causes auxin-transporting cells to become more efficient in auxin flux resulting in stable 'auxin canals'. The increased conductivity of these gradually restricted domains with high auxin levels not only leads to their vascular differentiation but also depletes neighboring cells of auxin preventing them from taking on a vascular cell fate (Avsian-Kretchmer et al., 2002; Mattsson et al., 1999; Rolland-Lagan et al., 2005; Sieburth, 1999). The transport capacity of the cells is due to the asymmetric distribution of PIN1 proteins whose expression in developing veins mirrors the pattern of auxin distribution predicted by the canalization model (Scarpella et al., 2006; Wenzel et al., 2007).

The positioning of PIN1 Expression Domains (PEDs) that will narrow to form veins is determined by the expression of PIN1 in the epidermal cells of the leaf

margin. Initially, the epidermal cells of the young leaf primordia have apical PIN1 localization directing the formation of auxin maxima at the leaf apex (Figure 1.4A) (Benkova et al., 2003; Reinhardt et al., 2003). The distal auxin maximum then induces PIN1 in the cells along the vertical axis of the primordium. The PED is initially wide but narrows to a file of cells with basal PIN1 localization, predicting the formation of the vascular strand of the midvein (Bayer et al., 2009; Hou et al., 2010; Scarpella et al., 2006; Wenzel et al., 2007). Concurrently, PIN1 polarity in the distal marginal cells shifts from apical to basal, establishing lateral auxin maxima on either side of the leaf (Friml et al., 2002; Scarpella et al., 2006). These lateral convergence points generate auxin maxima that control characters of leaf shape and vein pattern: 1) they induce leaf outgrowth to form serrations (Hay et al., 2006; Kawamura et al., 2010) and 2) they induce PIN1 in the adjacent ground meristem predicting the position of the secondary veins (Scarpella et al., 2006; Wabnik et al., 2010; Wenzel et al., 2007).

As in the midvein, during secondary vein formation PIN1 is initially expressed in a wide group of cells with symmetric localization and then narrows down to a single cell file with asymmetric localization (Hou et al., 2010; Scarpella et al., 2006; Wenzel et al., 2007). During the formation of the secondary vein loop, two domains with distinct PIN1 polarity appear: 1) the lower loop domain (LLD), associated with the lateral convergence point, forms first (Figure 1.4B). The cells in this domain have basal PIN1 localization directing auxin flux towards the proximal part of the midvein. 2) the upper loop domain (ULD) extends from the LLD to the distal midvein (Figure 1.4C). Cells in this domain have apical PIN1 localization and direct auxin flux

upwards into the midvein. Connecting the two domains is a cell with bipolar PIN1 localization on both apical and basal cell membranes (Scarpella et al., 2006; Wabnik et al., 2010; Wenzel et al., 2007). Failure to form bipolar cells is observed in mutants that show a disconnected vein network (Hou et al., 2010).

1.4 Transcriptional Regulation of PIN

I discussed in previous sections that the auxin level is regulated by changes in PIN polar localization. Further, changes in auxin levels are an important determinant of PIN expression and its localization (Peer et al., 2004; Vieten et al., 2005). This suggests that there is a feedback regulation between auxin levels and auxin transport. Auxin regulates the transcription of PIN and other auxin inducible genes by triggering the auxin response pathway that involves the signaling cascade of F-box protein TIR1 (Transport Inhibitor Response1) auxin receptor (Dharmasiri et al., 2005; Ruegger et al., 1998; Tan et al., 2007). When auxin concentration is high, it binds to the TIR1 auxin receptor. This event stimulates TIR1 to initiate proteolytic degradation of Aux/IAA proteins. Aux/IAA proteins are transcriptional repressors of auxin response factors (ARF). Proteolytic degradation of Aux/IAA derepresses ARF (Auxin Response Factors), which can now initiate the transcription of auxin inducible genes. In contrast, when auxin concentration is low, ARF is repressed by AUX/IAA and therefore no transcription occurs (Rogg and Bartel, 2001; Tiwari et al., 2001).

At the cellular level, the amount of PIN protein present at the plasma membrane depends on its vesicle-mediated cycling between the plasma membrane

and endosomal compartments versus its degradation at the vacuole (Abas et al., 2006; Dhonukshe et al., 2007; Geldner et al., 2001; Kleine-Vehn et al., 2008; Laxmi et al., 2008). I will first discuss the organelles and the machinery involved in vesicle trafficking of proteins in general, and then discuss what is known about PIN protein cycling and regulation of vesicle transport.

1.5 Vesicle trafficking

1.5.1 Organelles of the endomembrane system

Unlike prokaryotes, eukaryotic cells contain an elaborate system of membrane bound nucleus and other membrane bound structures in the cytoplasm called organelles or compartments. These organelles include Endoplasmic Reticulum (ER), Golgi apparatus, mitochondria, endosomes, peroxisomes and lysosomes (Bonifacino and Glick, 2004). Vacuoles, which perform the same degradation function as lysosomes in other eukaryotes are unique to plants and fungi. This group of organelles form the backbone of the endomembrane system. Since sorting and modification of proteins and other cellular compounds depend on this system, it provides a key control mechanism for protein trafficking (BarPeled et al., 1996; Muday et al., 2003).

The newly synthesized proteins enter the lumen of the ER. At the ER, these proteins are appropriately folded and glycosylated before being incorporated into anterograde transport vesicles and delivered to the Golgi apparatus (Cacan and Verbert, 2000). The Golgi apparatus is a stack (complex) of tubular cisternae. The ER derived vesicles fuse with the cis-Golgi (the region nearer to ER). During an event

called cisternal migration, the proteins contained in the cis-Golgi move to the trans-Golgi (the region away from the ER). Proteins at the Trans Golgi Netwok (TGN) carry distinct information and destination and therefore require sorting (Gu et al., 2001). Proteins that have ER retrieval signals are returned back to the ER from the Golgi *via* transport vesicles. The vesicle-mediated recycling of proteins from the destination organelle back to the originating organelle for further events of transport is known as retrograde transport (Bonifacino and Rojas, 2006). Proteins that are targeted for degradation are sorted into vesicles destined to lysosomes in animals or vacuoles in yeast and plants. Those that have extracellular and plasma membrane signals are dispatched into secretory vesicles, which in the process of exocytosis, are directed to fuse with the plasma membrane (Figure 1.5). After the fusion, the contents of the vesicle are deposited at the destination organelle/membrane (Burgoyne, 1990). Each of the transport events is highly specific to ensure that the cargo is sent to the correct destination at the right time (Bonifacino and Rojas, 2006).

1.5.2 Vesicle budding

Proteins travel between the organelles in coated vesicles. Vesicles bud at the originating organelle membrane and are consumed at the target organelle membrane. Vesicle budding starts with the assembly and polymerization of the coat proteins onto spherical or tubular buds at the membrane surface. This assembly helps collect membrane required for vesicle formation and also helps package specific cargos inside of the vesicles. After the vesicle bud is formed, it gets detached from the membrane (Bonifacino and Glick, 2004).

Based on their coat proteins, there are three types of coated vesicles: clathrin-coated vesicles that mediate transport from TGN and plasma membrane, and Cytoplasmic Coat ProteinI- (COPI-) and COPII-coated vesicles that mediate transport within the Golgi, from Golgi to ER and from ER to Golgi (Bonifacino and Glick, 2004). The major proteins of the clathrin-coated vesicles are clathrin and adaptin. The adaptin protein helps clathrin bind to the membrane and recruit cargo into the vesicles. The pinching off of the clathrin coated vesicle bud involves a GTP-binding protein called dynamin. Dynamin assembles around the neck of the bud and helps it detach from the membrane surface (Brodsky et al., 2001; Robinson, 1994).

Monomeric GTPases function at various stages of vesicle transport. They cycle between inactive, GDP (Guanosine Diphosphate)-bound, and an active, GTP (Guanosine Triphosphate)-bound form. The switch between active and inactive forms, which is mediated by Guanine nucleotide Exchange Factor (GEF) and GTPase Activating Protein (GAP), is an important conformational change to regulate various steps of vesicle cycling (Geldner et al., 2001; Surpin and Raikhel, 2004). There are 5 families of the small GTP binding proteins (G protein) superfamily namely: ADP-Ribosylation Factor (Arf)-GTPase/Secretion-Associated Ras1 (Sar1)-GTPase, Ras-GTPase, Ras related Nuclear (Ran)-GTPase, Rho-GTPase and Rab-GTPase (Takai et al., 2001). Among these, Sar1-GTPase, Arf-GTPase and Rab-GTPase are involved during different stages of vesicle cycling. Sar1-GTPase and Arf-GTPase provide specificity to the coat assembly by specific recruitment of the coat to determine the destination vesicle. They also regulate the disassembly of the coat proteins. The disassembly of coat proteins after budding is a prerequisite for the fusion event of

the vesicle at the target membrane (Bonifacino and Glick, 2004; Takai et al., 2001). The Rab-GTPase family discussed in the following section is involved in vesicle fusion events.

1.5.3 Vesicle fusion

For the cargo to be consumed at the target membrane, vesicles require the fusion machinery. Membrane fusion is accomplished by coordinated action of a) tethering complexes, b) Soluble *N*-ethylamide-sensitive factor Attachment protein Receptors (SNAREs) and c) small GTPases.

a) Tethering complexes: Tethering is the initial physical event that links two participating membranes before the fusion. Based on structure, tethering complexes are of two types: coiled-coil and multisubunit tethering complex (Cai et al., 2007; Whyte and Munro, 2002). These complexes are conserved among eukaryotes and reside on specific cellular compartments. Based on studies from yeast, TRAnsport Protein Particle 1 (TRAPP1) tethers vesicles at the Golgi originating from the ER, TRAPPII transports cargos within the Golgi, exocyst tethers Golgi derived vesicles at the PM, Homotypic vacuole fusion and vacuole Protein Sorting (HOPS) tethers endocytosed vesicles at the PVC or vacuole, Golgi Associated Retrograde Protein (GARP) tethers late endosome (LE) derived vesicles at the TGN and finally Dependence on SLy1-20 (DSL1) tethers vesicles derived from the Golgi at the ER (Koumandou et al., 2007; Lupashin and Sztul, 2005).

b) SNAREs: Specificity of the membrane fusion is provided by SNARE family. SNAREs are mostly cytosolic transmembrane proteins and exist as cognate pairs;

vesicle membrane SNAREs (v-SNAREs) and target membrane SNAREs (t- SNAREs). These complementary SNAREs have helical domains necessary for complex formation that draws the vesicle membrane in proximity to the target membrane and facilitates fusion. After the fusion event, the v-SNARE – t-SNARE complex dissociates and the v-SNARE is able to return back to the originating organelle to get repackaged into vesicles (Bonifacino and Glick, 2004; Chen and Scheller, 2001).

c) Small GTPases: Rab-GTPases work together with other proteins to orchestrate multiple steps during the fusion events (Takai et al 2001). Rab proteins are incorporated in the v-SNARE of the transport vesicle and provide its specificity for recognition of the correct t-SNARE and hence deliver the cargo to the membrane of the correct organelle (Takai et al 2001). Rabs are also known to be involved in initial recruitment of the tethering factors to the membrane (Cai et al., 2007). Rabs converted to their active GTP bound form can bind to the tethering factors and initiate the fusion. After the fusion event, Rab is inactivated to the GDP bound form (Cai et al., 2007).

1.6 Endocytosis

1.6.1 Plasma membrane proteins are endocytosed and recycled

In a process opposite to exocytosis, plasma membrane proteins undergo endocytosis (Figure 1.5). Endocytosis refers to uptake of extracellular substance or internalization of plasma membrane protein followed by transport to the endosomes (Besterman and Low, 1983). By regulating the amount of proteins present in the plasma membrane, endocytosis helps to maintain key cellular processes such as cell

polarity and signal transduction, cytokinesis and nutrient uptake (Sorkin and von Zastrow, 2002; Surpin and Raikhel, 2004).

Clathrin coated vesicle mediated endocytosis contributes to bulk endocytosis (Dhonukshe et al., 2007). The first destination of these endocytosed vesicles is the endosomes where major sorting events take place. Broadly, endosomes are of two types, the early endosomes and the late endosomes. The early endosome is generally where the endocytosed plasma membrane protein is first delivered and sorted for further transport (Figure 1.5).

Depending on the destination, the sorted cargo can be routed to either the lysosome for degradation or to recycling endosomes, which shunt proteins back to the plasma membrane. For recycling of proteins to the plasma membrane, the sorted cargo is delivered to the plasma membrane through recycling endosomes (Bonifacino and Glick, 2004). In plants, the structural and functional organization of early endosomes is different. As revealed by studies using FM4-64, a lipophilic styryl dye that traces the endocytic pathway (Geldner et al., 2003), the TGN itself acts as the early endosome in plant cells (Dettmer et al., 2006; Oliviusson et al., 2006; Paciorek et al., 2005). Moreover, while the sorting of the endocytosed proteins in animals and yeast occurs at the early endosme, in plants it occurs at the TGN. The TGN in a plant cell is therefore a sorting station for both endoplasmic reticulum derived proteins and plasma membrane derived endocytosed proteins (Viotti et al., 2010). This implies that the sorting event at the plant TGN is more complex and needs to be precisely regulated.

1.6.2 Some of the endocytosed proteins are targeted for degradation

The late endosomes are Multivesicular Bodies (MVB) that in the plant cell is sometimes called the Pre-Vacuolar Complex (PVC) (Oliviusson et al., 2006). These are the intermediate organelles that receive the vesicles with cargo sorted for degradation (Robinson et al., 2008; Viotti et al., 2010). These proteins are incorporated into the lumen of the vesicles of the multivesicular bodies that transport them to the lysosome. The internalization of the proteins into the lumen is mediated by Endosomal Sorting Complex Required for Transport (ESCRT) machinery (Katzmann et al., 2001; Katzmann et al., 2003; Spitzer et al., 2009). Finally, the vesicles with cargo destined for degradation are targeted to lysosomes. Lytic vacuoles in yeast and plants are equivalent compartments to animal lysosomes with respect to protein degradation. In addition to the lytic vacuole, plants also contain protein storage vacuoles (Vitale and Hinz, 2005), the protein reservoirs, which can be used during different phases of growth, for example during seed germination.

Proteins targeted for the lysosome are first recognized by Vacuolar Sorting Receptors (VSRs) before they are sorted into vesicles. Studies in yeast and mammals show that VSRs cycle continually between late endosome and TGN. The efficiency with which proteins are targeted to lysosome/vacuole is determined by the rate of recycling of VSR between LE and TGN (Bonifacino and Rojas, 2006). Mannose 6-phosphate receptor (Braulke and Bonifacino, 2009) and Vacuolar Protein Sorting 10 (VPS10) are well known examples of TGN localized receptors in yeast and mammals, respectively (Bowers and Stevens, 2005; Marcusson et al., 1994).

The recycling of the VSRs between the late endosome and the TGN involves two important complexes, the GARP complex and the retromer complex.

1.6.2.1 The GARP complex

GARP is a tetrameric tethering complex consisting of Vacuolar Protein Sorting 51 (VPS51), VPS52, VPS53 and VPS54 subunits and is important for maintaining proper lysosome function. The role of GARP complex in retrieval of a number of lysosomal/vacuolar sorting receptors at the TGN has been well demonstrated in *Caenorhabditis elegans*, yeast and mammals. In yeast, it tethers late endosome derived vesicles at the TGN, allowing retrieval of vacuolar cargo receptors and processing enzymes (Conibear et al., 2003; Conibear and Stevens, 2000; Reggiori et al., 2003; Siniossoglou and Pelham, 2002; Siniossoglou and Pelham, 2001). In humans and *C. elegans* also the GARP complex functions in retrieval of lysosomal cargo receptors and defects to GARP components affect the sorting of lysosomal proteins (Luo et al., 2011; Pérez-Victoria et al., 2008; Pérez-Victoria et al., 2010b). The GARP complex has a critical function in metazoan development since mutation to VPS54 causes embryonic lethality, a neuron degeneration phenotype and sperm defects in mice as well as motility and male transmission defects in *C. elegans* (Luo et al., 2011; Pérez-Victoria et al., 2010a; Schmitt-John et al., 2005).

The GARP complex is evolutionarily conserved and present in all eukaryotes (Koumandou et al., 2007). Mutations in three subunits (VPS52, VPS53 and VPS54) of the GARP complex have been identified in *Arabidopsis* and are associated with male transmission defects during fertilization (Guermonprez et al., 2008; Lee et al., 2006;

Lobstein et al., 2004), heat tolerance defects during seedling growth (Lee et al., 2006; Wang et al., 2011; Wu et al., 2000) and sensitivity to osmotic stress (Lee et al., 2006). These defects suggest that, as in metazoans, the GARP complex has an important developmental role in plants.

1.6.2.2 The retromer complex

In addition to the GARP complex, the retrograde transport from late endosomes to TGN involves a multisubunit complex called the retromer complex. In yeast this complex consists of 5 subunits: VPS5, VPS17, VPS26, VPS29 and VPS35 (Seaman et al., 1998). VPS5 and VPS17 are orthologues to mammalian Sorting Nexin-1 (SNX1) and SNX2 respectively. In mammals the pentasubunit retromer complex is organized into two subcomplexes: a dimer of SNX1 and SNX2, and a trimer of VPS26, VPS29 and VPS35 proteins. During the transport event, the dimer is proposed to recruit the complex to the late endosomes, and the trimer binds the cargo (Bonifacino and Rojas, 2006; Seaman, 2005).

Structurally the plant retromer resembles that of yeast and animals. Its localization at the PVC in *Arabidopsis* and tobacco BY-cells (Jaillais et al., 2008; Oliviusson et al., 2006; Yamazaki et al., 2008) is consistent with its role in recycling of VSR from PVC/late endosomes to TGN (Shimada et al., 2006; Yamazaki et al., 2008). In *Arabidopsis,* mutations in the subunits SNX1 and VPS29 show auxin transport related defects such as loss of gravitropism and reduced growth (Jaillais et al., 2006; Jaillais et al., 2007; Kleine-Vehn et al., 2008; Yamazaki et al., 2008) suggesting that the retromer complex may be involved in regulating the auxin

transport machinery and may have an important role in plant development.

1.7 Mechanism and components of PIN protein localization

Newly synthesized PIN proteins are sorted at the TGN and canonically targeted to the plasma membrane. Depending on cell type and the PIN protein involved, PIN proteins can be targeted to the apical, basal or lateral side of the cell.

Depending on intrinsic and external signals, PIN proteins show dynamic changes in localization at different faces of the cell as well as at different regions within the same face (Friml et al., 2004; Li et al., 2011). Such changes in PIN localization provide an opportunity to integrate multiple signals within the single cell and regulate the directional flow of auxin. The antagonistic actions of PINOID, a serine threonine kinase, and of protein phosphatase 2A mediate PIN polarity (Friml et al., 2004; Michniewicz et al., 2007).

In the earlier sections of this chapter we saw that PIN localization is important for establishing the auxin gradient responsible for root meristem specification. The basal localization of PIN proteins during the embryonic globular stage results in auxin accumulation in the hypophysis (Friml et al., 2003) (Figure 1.2). Overexpression of PID, at this stage, switches basal localization of PIN to apical localization. The basal-apical switch reverses the auxin flow towards the upper cells instead of the hypophysis leading to loss of root-shoot polar axis and bilateral symmetry of the cotyledons. Similarly, overexpression of PID in root during post-embryonic development results in basal–apical PIN polarity and therefore a reduced auxin maximum at the root meristem (Friml et al., 2004).

Counterbalancing the activity of PID is the protein phosphatase PP2A. While PID phosphorylates PIN, PP2A dephosphorylates it (Christensen et al., 2000; Michniewicz et al., 2007). Loss of function *pp2a* embryo and root show similar defects as seen in PID over expression lines (Friml et al., 2004; Michniewicz et al., 2007). Recent studies have revealed that PIN1 phosphorylation status is important for guard cell polarity and interdigitated pattern of pavement cells (PC) in leaves and cotyledons (Li et al., 2011). In guard cells, PID overexpression led to a PIN1 switch from the inner plasma membrane to the outer plasma membrane. In PC, *PID* over expression induced PIN1 polarity shift from lobes to indentations similar to the effect seen in a mutant encoding the member of PP2A family. These results led to the proposal that hypo-phosphorylated PIN1 is largely in the lobes and hyper-phosphorylated PIN1 in the indentations (Li et al., 2011).

Thus the phosphorylation status of PIN, which switches PIN localization between different faces of the cell in the embryo and root or between different regions within the same face of a single cell such as in pavement cells has a profound impact on auxin transport and therefore on cell and tissue patterning.

1.7.1 PIN is endocytosed and recycled back to the membrane

The plasma-membrane-localized PIN proteins are known to undergo endocytosis followed by continuous recycling between the plasma membrane and endosomal compartments *via* recycling vesicles and/or targeting to vacuole for degradation *via* the pre-vacuolar complex, the late endosomes.

Application of Brefeldin A (BFA) has been routinely used to show that PIN proteins are recycled back to the plasma membrane (Geldner et al., 2003; Geldner et al., 2001; Steinmann et al., 1999). BFA is a fungal toxin that inhibits the transport of proteins to the plasma membrane and is reversible upon washing. This reversible blockage by BFA causes endosomes containing the PM targeted cargo vesicles to accumulate into BFA compartments. It turns out that BFA targets GNOM. GNOM is a BFA sensitive, plant-specific Arf-GTPase and is required to traffic PIN from endosome to the plasma membrane (Steimann et al 1999, Dhonuske et al., 2007, Geldner et al 2001, 2003). Consistent with the role of GNOM in polarized PIN1 localization, *gnom* mutants show embryonic defects including loss of apical basal polarity of the embryos. *gnom* phenotypes can be phenocopied by treating seedlings with BFA (Geldner et al., 2001; Steinmann et al., 1999).

A series of experiments (Dhonukshe et al., 2007) using fluorescent markers provided direct evidence for endocytosis and recycling of PIN proteins. They used a PIN2:Green Fluorescent Protein (GFP) fusion line to monitor PIN2:GFP dynamics in the root epidermis and compared this with the endocytosis of FM4-64. The overlapping of the internalized PIN2:GFP with FM4-64 suggested that PIN2 undergoes endocytosis. To investigate whether the endocytosed PIN2 returns back to the plasma membrane, they used PIN2:EoSFP, a photoconvertible PIN2 construct that turns green to red when induced by UV. To better visualize the internalized PIN2 they used BFA and inhibited the recycling of PIN2:EoSFP containing endosomes back to the plasma membrane. They showed that the photoconverted PIN2:EoSFP accumulated in BFA compartments along with its non-converted form

PIN2:GFP. These compartments disappeared upon BFA washout and PIN2:EoSFP and PIN2:GFP reappeared at the plasma membrane (Dhonukshe et al., 2007). These results suggested that PIN2 is endocytosed from and recycled to the plasma membrane.

Clathrin-coated vesicles mediate endocytosis of PIN. By using a series of elegant cell biology and molecular tools, Dhonukshe et al., (2007) visualized clathrin and clathrin-coated pits at the plasma membrane and demonstrated that PIN proteins are internalized into clathrin-coated vesicles for their endocytic delivery to the endosome. In support, treatment of PIN2:GFP roots with tyrphostin A23, an inhibitor of recruitment of endocytic cargoes into the clathrin mediated pathway, prevented endocytosis of PIN2 (Dhonukshe et al., 2007).

Auxin regulates the abundance of PIN at the plasma membrane by inhibiting its endocytosis (Paciorek et al., 2005). Even low concentrations of exogenously applied auxin showed a pronounced reduction of FM4-64 uptake from the plasma membrane in *Arabidopsis* root (Paciorek et al., 2005). The same was true for uptake of FMI-43, another endocytic tracer, in tobacco BY-2 suspension cells (Paciorek et al., 2005). Furthermore, roots of the *Arabidopsis* auxin synthesis mutant *yucca*, which has higher concentrations of endogenous auxin, also showed reduced FM4-64 uptake. *tir3* mutant alleles showed a reduced inhibitory effect of auxin on PIN1 and PIN2 uptake when compared to wild type (Paciorek et al., 2005). The *tir3* mutant was originally isolated in a genetic screen for plants showing resistance to auxin transport inhibitors (Ruegger et al., 1998) and *tir3* alleles were later found to show resistance to the effect of auxin on endocytosis (Paciorek et al., 2005). These results

suggested that auxin affects endocytosis of at least PIN1 and PIN2 such that when auxin concentrations are high, PIN level at the plasma membrane is increased, resulting in increased auxin transport.

1.7.2 PIN is endocytosed and targeted for vacuolar degradation

In addition to being recycled, PIN proteins are also targeted for vacuolar degradation at the lytic vacuole. The endocytic tracer FM4-64 is also used to visualize endocytic movement of PM proteins to the vacuole. FM4-64 is time and temperature dependent and stains the vacuolar membrane in 60 min at 30°C (Vida and Emr, 1995). Experimental observations reveal that PIN proteins colocalize with FM4-64 suggesting that at least a portion of PM-localized PIN proteins are continuously endocytosed and targeted for vacuolar degradation (Oliviusson et al., 2006). Elegant biochemical experiments have shown that PIN proteins are transported to the vacuole from the TGN through PVC (Kleine-Vehn et al., 2008; Laxmi et al., 2008; Oliviusson et al., 2006; Spitzer et al., 2009). The vacuolar degradation pathway involves similar complexes as lysosomal targeting in other eukaryotes. Mutation in genes encoding ESCRTs (Spitzer et al., 2009), Adaptor Protein 3 (AP3) subunits (Feraru et al., 2010), Vacuolar Morphology 3 (VAM3) (Shirakawa et al., 2009), all homologues to components known to have a role in lysosomal targeting in other eukaryotes, have defects in localization of PIN protein in the plasma membrane often accompanied by its ectopic accumulation within the cytoplasm. These defects are reflected in plant phenotypes including leaf vein

formation defects indicating an important regulatory role for vacuolar targeting of PIN during plant development.

1.7.3 Retrograde trafficking of PIN

A balance between how much PIN is degraded and how much is recycled is established in order to control how much auxin is transported. One example of this dynamic balance is shown during sudden changes to external stimulus such as light or gravity. For instance, when a vertically grown root is rotated by 90 degrees, the file of epidermal cells up the gravitational gradient shows increased degradation of PIN2 such that their auxin transport is reduced compared to the file of cells down the gradient (Kleine-Vehn et al., 2008). This difference in auxin transport is required for bending of the root towards gravity. When the gravity stimulus is prolonged and bending is complete, the amount of PIN2 being degraded on the cells up the gravitational gradient is reduced. This rapid reduction is due to a specific pathway that involves retrograde trafficking of PIN2 from the PVC to the recycling endosomes or TGN. This pathway involves SNX1, a component of the plant retromer complex (Kleine-Vehn et al., 2008). As such, *snx*-1 mutants show gravitropic defects (Jaillais et al., 2008; Jaillais et al., 2007; Kleine-Vehn et al., 2008).

Previous studies reported the involvement of VPS29, another component of the retromer complex in recycling of endosomal PIN to the plasma membrane (Jaillais et al., 2007) however it was not clear whether the compartments to which VPS29 localized is the PVC or the early endososme equivalent TGN. A recent study (Niemes et al., 2010) suggests that components of the plant retromer complex reside

at the TGN and are required to recycle VSRs in and out of the TGN. When they examined the protoplasts of tobacco *snx* mutants, they found elevated levels of VSRs at the TGN. This is consistent with the earlier studies (Shimada et al., 2006; Yamazaki et al., 2008) that suggested the role of retromer in recycling of VSRs between TGN and PVC in plants. Despite the conflicting views regarding the localization of the retromer complex, it appears in general to be involved in two functions: 1) retrograde transport of PIN proteins from PVC to recycling endosomes or the TGN during differential gravitropic response and 2) recycling of VSRs between TGN and PVC during vacuolar targeting of PM proteins. The involvement of the retromer complex in PIN localization suggests that other components of retrograde trafficking such as the GARP complex may also have a role.

1.8. Objectives

In the first part of the introductory chapter, I reviewed evidence that the asymmetric localization of PIN proteins controls directionality of auxin transport and many aspects of plant development. In the second part I discussed how asymmetric localization of PIN proteins at the plasma membrane, a regulated process, is mediated by vesicle cycling. The overall objective of the thesis is to understand how the *Arabidopsis* gene *UNHINGED*, which I show is a component of the GARP complex, affects PIN1 levels at the plasma membrane and hence controls auxin-transport-regulated developmental processes including leaf vein patterning, leaf shape, leaf cell interdigitated patterning and root growth.

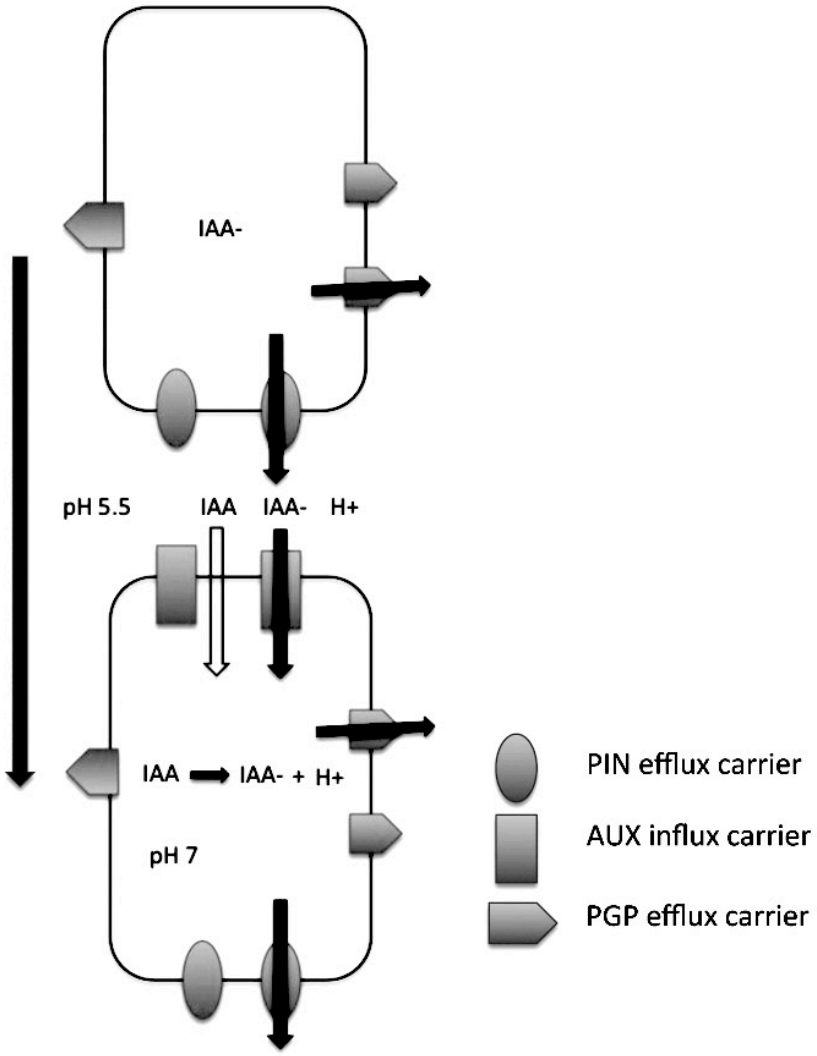

Figure 1.1: The chemiosmotic model for polar auxin transport.
Auxin (IAA) exists in undissociated and dissociated forms in the acidic environment (pH 5) of the apoplast. Due to pH differences between the apoplast and cytosol (pH 7) IAA can diffuse through plasma membrane (white arrows). The transport of IAA- (black arrows) inside the cell requires AUX1 influx carriers at the plasma membrane. In the cytosol, IAA dissociates and requires the activity of efflux carriers (PGP and PIN) to exit out of the cell. Localization of efflux carriers determines the directionality for the major flux of auxin (shown as a long arrow). PGP shows apolar localization and PIN shows localization to a specific face of the cell.

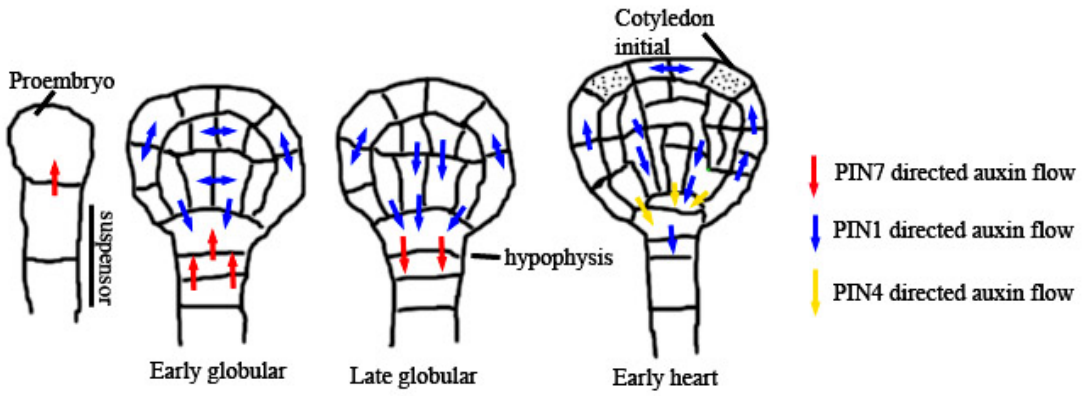

Figure 1.2: Directionality of auxin flow during *Arabidopsis* embryogenesis. Changing flows of auxin (arrows) due to localization and dynamic relocalization of PIN1, PIN4 and PIN7 proteins. Between early and late globular stages PIN1 and PIN7 undergo a polarity switch. At the late globular stage PIN1 and PIN4 contribute to auxin maxima of the hypophysis. PIN1 in the epidermal cells of the early heart stage contribute to auxin maxima for cotyledon initials. The late globular and early heart stages are simplified with fewer cells and successive stages are not to scale. Redrawn from Feraru and Friml, (2008)

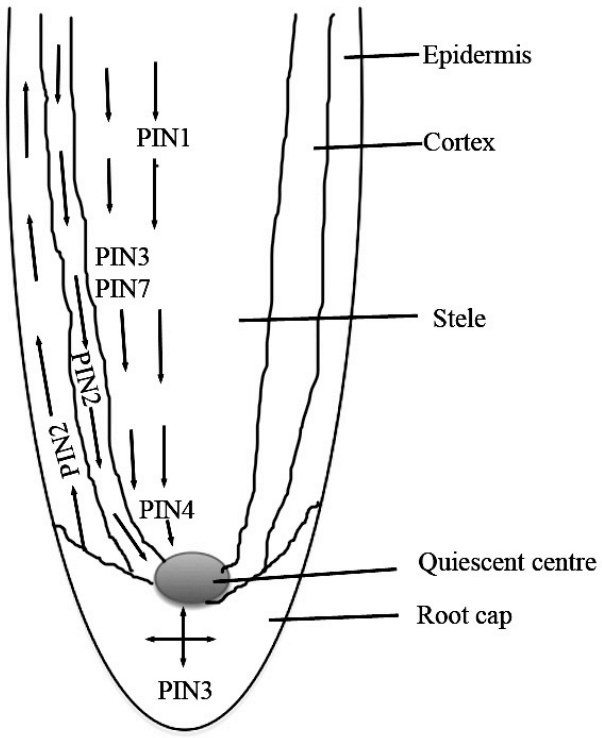

Figure 1.3: Directionality of auxin flow in the *Arabidopsis* root.
Auxin flow (arrows) mediated by asymmetric localization of PIN proteins in different regions of the root (apical localization of PIN2 in the epidermis and basal in cortex, basal localization of PIN1, PIN3, PIN4 and PIN7 in the stele and asymmetric localization of PIN3 in the columella and root cap). Auxin flow in one half of the root is shown for convenience. The quiescent centre denotes the region of auxin maxima in root. Adapted from Petrasek and Friml, (2009)

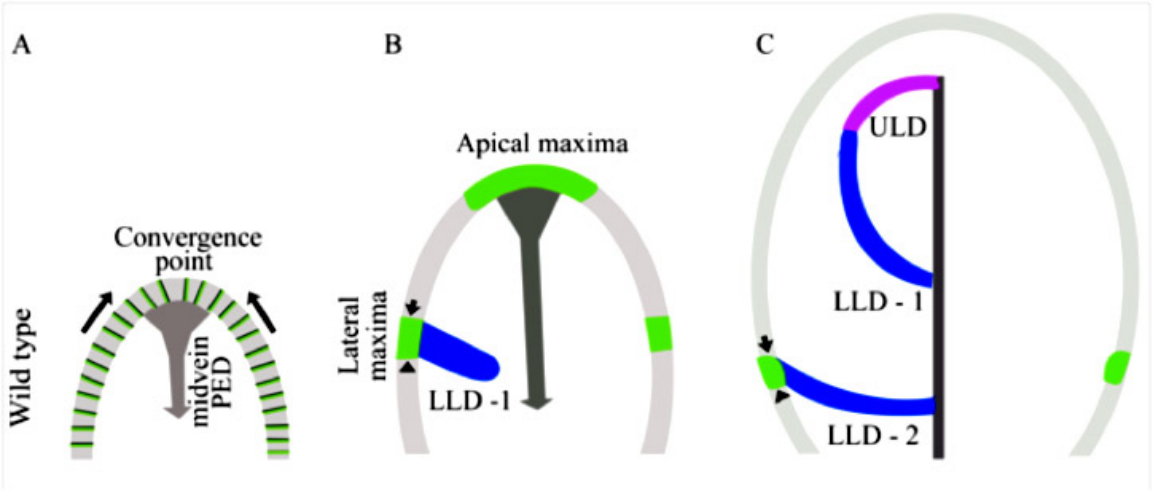

Figure 1.4: PIN1 localization, auxin maxima formation and leaf vein formation during early stages of the *Arabidopsis* first leaf.
At early stages PIN1 is localized apically (green) on all epidermal cells generating a convergence point (a region for auxin maxima) towards the apex (arrows in A). The auxin maximum generates the midvein PED that is wide distally and narrows proximally (Dark grey in B). Lateral margin maxima are positioned on the margin due to PIN1 polarity switch in cells distal to the new maxima (arrow above lateral maxima) and generation of new PED (arrowhead below lateral maxima). The lateral maxima initiate LLD - 1 of the first set of secondary veins (blue in B). At subsequent stages LLD-1 is extended and the PED is completed distally by the ULD (magenta in C). The shift in lateral maxima proximally generates LLD-2 to initiate a second set of secondary veins. Adapted from Scarpella et al., (2006).

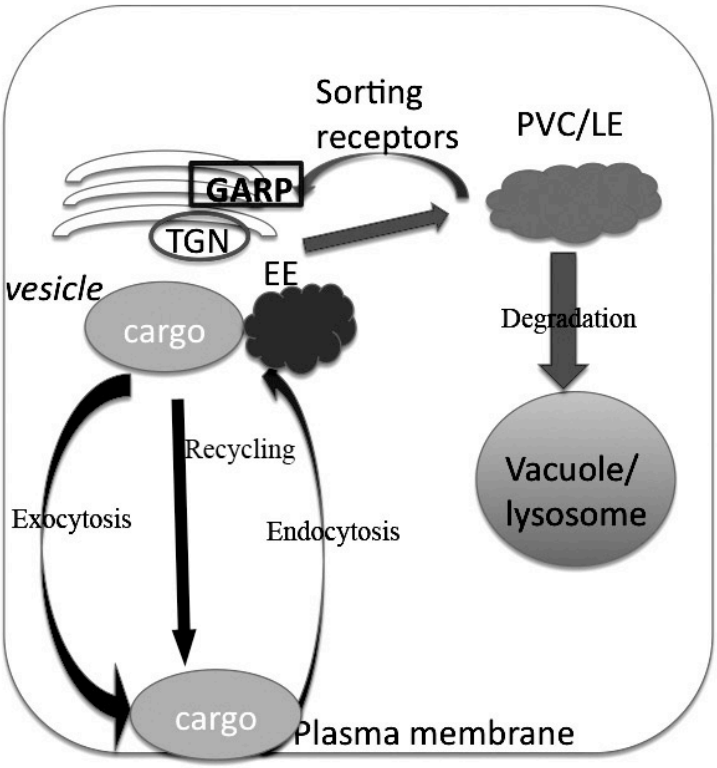

Figure 1.5: Simplified scheme for general mechanism of vesicle cycling. Plasma membrane proteins cargos sorted at the Trans Golgi Network (TGN) are exocytosed. Some of the plasma membrane proteins are endocytosed to early endosomes (EE) /TGN . These proteins can undergo degradation in the vacuole/lysosome via late endosome (LE)/PVC, or be recycled back to plasma membrane. The degradation requires proteins be recognized by vacuolar sorting receptors. The sorting receptors cycle between LE and TGN. The tethering of the receptors at the TGN is facilitated by the GARP tethering complex. All arrows refer to trafficking of cargo proteins.

CHAPTER 2: MATERIALS AND METHODS

2.1 Accession Numbers

DNA Sequence data used in the study can be found in The Arabidopsis Information Resource (TAIR) database under the following accession numbers: *UNH/VPS51* (At4g02030), *VPS52* (At1G71270), *VPS53/HIT1* (At1G50500), *VPS54* (At4G19490), *VAM3* (At5g46860), *VTI11* (At5g39510), *TLG2A* (At5g26980), *YPT6* (At2g44610), *SYP61* (At1g28490).

2.2 Seeds and cloning vectors

Arabidopsis thaliana, Columbia (Col-0) ecotype, was used as a wild type control in all experiments and as a background for all the mutants. Ethyl methane sulfonate (EMS) treated lines of *Arabidopsis* were obtained from Lehle Seed (Round Rock, TX, USA). *pin1-1* seed was from Thomas Berleth (University of Toronto, Toronto, ON), *DR5:GUS* from Jane Murfett (University of Missouri, Columbia, MO), *vam3-4* seeds from Taku Takahashi (Ohtomo et al., 2005) and *vti11* seeds from Miyo Morita (Kato et al., 2002). *PIN1:GFP, ATHB8*:*GUS, aux1-7, eir1-1* were from the Arabidopsis Biological Resource Centre (ABRC), OH. The T-DNA insertion line GABI_520G08 was obtained from GABI-kat (Kleinboelting et al., 2012). CloneJet (pJET1.2/blunt) vector was from from Fermentas Lifesciences and the vectors pGreen229 (Hellens et al., 2000) and pBI:GUS (pBI101.2) were obtained from Shelly Hepworth, Carleton University, SYP61:YFP from Luciana Renna (Stefano et al., 2010), and pVKH18:GFPN from Hugo Zheng, McGill University.

2.3 Growth conditions for *Arabidopsis*

Seeds were planted either on a mixture of ¾ Flora Compo compost (The Professional Gardener Co Ltd., Calgary AB) and ¼ vermiculite (Coaldale Nurseries, Coaldale, AB) in 100 cm^2 pots or on Petri dishes containing *Arabidopsis thaliana* (AT) growth medium (Ruegger et al., 1998). Pots were covered with saran wrap and both pots and dishes were incubated at 4°C in the dark for 3 days, after which they were transferred to growth chambers (Percival Scientific, Perry, IA) with 24 hours of light at an intensity of approx. 130 μmol of photons per m^2 per sec. from Sylvania Cool White, Grow Lux, and incandescent bulbs (Osram Sylvania Inc, Danvers, MA). Chambers were set at 21°C and 60% relative humidity. The day of transfer to the growth chambers was considered to be the day of germination or 0 Days After Germination (DAG). Saran wrap was removed at 7 DAG and plants were maintained under constant growth conditions.

2.4 Growth conditions for Tobacco

Tobacco plants were grown at Michigan State University by Dr. Elizabeth Schultz using the following conditions*: Nicotiana tabacum* SR1 (cv Petit Havana) seeds were disinfected with 70% ethanol before plating on Murashige and Skoog basal salt medium (Sigma) containing 0.8% agar (Difco). The plates were incubated for 2 weeks at 20-22°C after which the seedlings were transferred to soil and maintained at 21°C long day (16 hour light, 8 hour dark) conditions.

2.5 Transformation and growth of *Escherichia Coli* DH5α and *Rhizobium radiobacter* GV3101

The subcloning efficiency *E. coli* strain DH5α was obtained from Invitrogen and transformation was performed following the manufacturer's protocol except that heat shock was performed for 45 seconds instead of 20 seconds. The transformed cells were plated onto LB media supplemented with the appropriate antibiotic (50 μg/mL kanamycin or 100 μg/mL of ampicillin) and incubated at 37°C for 16 hrs.

Transformation of a binary vector into the electro competent *Agrobacterium* strain GV3101 was performed as follows. About 2 μg of vector DNA was added to 80 uL of thawed *Agrobacterium* cells. To facilitate the electroporation of pGreen 229 vector in GV3101, 1 μg of p-SOUP DNA was also added to the thawed cells. The reaction mixture was ice-chilled for 3 min, and transferred to an ice-chilled electroporation cuvette. The cuvette was placed in the electroporator (Eppendorf electroporator 2510) and electroporation was performed at 2.5kV. 1mL of LB medium was added to the electroporated cells which were incubated on a shaker (200 rpm) at 28°C for 2 hours to allow recovery and expression of antibiotic resistance markers. 200μL of transformed cells were plated onto LB media supplemented with appropriate antibiotics (25μg/mL rifampicin and 25μg/mL gentamycin to select for *Agrobacterium* and 50μg/mL kanamycin to select for vector) and incubated at 28°C for 48-72 hrs for colonies to grow.

2.6 Transformation of *Arabidopsis* by floral spray method

A single positive colony of transformed *Agrobacterium* inoculated into 5 mL of LB with appropriate antibiotic was grown overnight on a 200 rpm shaker at 28°C. 1mL of this overnight culture was inoculated in 100 mL of LB medium with appropriate antibiotics and grown overnight under the same conditions. To harvest the cells, the overnight culture was centrifuged at 8000 rpm for 5 minutes and the pelleted cells were resuspended in 100 mL of freshly prepared 5% sucrose. The resuspended cells were centrifuged again under identical conditions and the pellets were resuspended in 200ml of 5% sucrose. 50μL of Silwet, a wetting agent (Silwet L-77, Lehle Seeds USA), was added to the resuspended cells before spraying liberally onto plants at the stage of flowering (approximately 25-30 DAG) (Hooker et al., 2007). Transformed plants were covered with plastic overnight. The second round of plant spraying was done after 7 days. Seeds were harvested when ready.

2.7 Identification and mapping of *unh-1*

The *unh-1* mutant is one of several identified in a previous screen (Steynen and Schultz, 2003). The mutant line was backcrossed to wild type at least four times prior to all analyses. To map *unh-1*, the mutant was crossed to Landsberg *erecta* (Ler) and DNA from young leaves was extracted (Dellaporta et al., 1983) from a population (n=230) of F2 plants showing *unh-1* mutant phenotype. Simple Sequence Length Polymorphisms (SSLPs) and Single Nucleotide Polymorphisms (SNPs) between Col-0 and Landsberg (Ler) in the flanking regions of chromosome 4 were

identified through the Cereon polymorphism database (Jander et al., 2002). The location of *unh-1* mutation was restricted to 15 candidate protein-coding genes in chromosome 4 by Ryan Cormark, a previous graduate student in the lab (Cormark, 2006). Sequencing of the candidate genes, which was done by Mike Blackshaw, a previous undergraduate student in the lab (Blackshaw, 2008), revealed a mutation in At4g02030.

2.8 Generation of transgenic constructs for plant transformation

To generate the complementation construct (*pUNH*), 10kb of wild type genomic sequence including 5000 bp upstream from the putative At4g02030 translation start site and 425 bp downstream from the putative translation termination site was amplified from wild type genomic DNA using gene specific primers new10_unhG_F and new10_unhG_R (Table 2.1) and products introduced into pJET1.2/blunt. *E. coli* DH5α colonies were screened for insertion by restriction analysis. Vectors containing the correct insertion were restricted with *NotI*, DNA was subjected to gel electrophoresis, and inserted DNA was extracted from the gel using a gel extraction kit (Bio Basic Inc.) according to the manufacturer's instructions. The insertion was then ligated into *NotI* sites of the pG229 II binary vector (Hellens et al., 2000) using T4 ligase.

For generating GUS reporter gene construct *(pBIUNH:GUS)*, the 5 kb upstream region was amplified with primers new5_unh_promo_F and new5_unh_promo_R (Table 2.1) and subcloned first into into pJET1.2/blunt as described for *pUNH* and

finally into the *XmaI* cloning site upstream of the *GUS* reporter gene of *pBI:GUS* binary vector.

To generate 35S:GFP:UNH construct, UNH cDNA was amplified From RAFL16-14-018 (pda19438, Riken BioResource Centre, Japan) using the primers UNH_GFPN_SalI_F and UNH_GFPN_STOP_SalI_R (Table 2.1) and ligated into the *SalI* sites of binary vector pVKH18:GFPN *via* pJET1.2/blunt as described for *pUNH* . The construct is such that GFP is at the N-terminal of the UNH translational start codon.

pBIUNH:GUS and *pUNH* were electroporated into *Agrobacterium* (GV3101) cells and were used to transform wild type plants and plants homozygous for the *unh-1* mutation respectively using the floral spray method (Hooker et al., 2007). The T1 transformants were identified by resistance to BASTA (Bayer Crop Science, 1 μL/mL) on soil for *pUNH* and resistance to 25 μM kanamycin on plates for *pBIUNH:GUS*. Multiple T2 lines of *pBIUNH:GUS* showing 100% resistance to selection markers were screened and a representative T3 line was used for analysis.

2.9 Transgenic lines, Gabikat line and generation of double mutants

The transgenic lines *unh-1 DR5:GUS* and *unh-1 ATHB8:GUS* and the double mutants *unh-1 pin1-1*, *unh-1 eir1-1* and *unh-1 aux1-7* were previously generated in the lab (Cormark, 2006). Double mutants were also generated between *unh-1* and *vam3-4* or *vti11.* Homozygosity of *vam3-4* in the double mutants was confirmed by genotyping using primers, vam3-4_F and vam3-4_2_R (Table 2.1), specific to the *vam3*-4 insertion. Homozygosity of *vti11* deletion was confirmed as previously described (Shirakawa et al., 2009). Homozygosity of *unh-1* was confirmed using

dCAPS primers, unh_dCAPS_R_BsmAI_F and unh_dCAPS_R_BsmAI_R (Table 2.1). *BsmA1* gives 251 + 29 bp and 280 bp amplicon lengths for wild type and *unh-1* respectively.

Homozygous F4 generation plants were used for analysis. Genotyping of Gabikat, T-DNA insertion line in At4g02030 (GABI_520G08), was performed by PCR using the primer set UNH_GABI_genespecific and UNH_GABI_PCR (Table 2.1). Plants homozygous for GABI_520G08 were crossed to *unh-1* and allelism was confirmed by non-complementation in F1 plants.

2.10 *GUS* staining and phenotypic analysis

GUS staining and clearing of cotyledons and leaves was performed as described previously (Kang and Dengler, 2002). Dissection and analysis of 14 DAG cotyledon and 21 DAG leaf vein phenotypes and expression analysis of *DR5:GUS, ATHB8:GUS, pBIUNH:GUS* was done as described previously (Steynen and Schultz, 2003). Auxin response of *pBIUNH:GUS* was examined following growth on media supplemented with 10^{-7}M 2,4-D. The area, perimeter and undulation index (Minamisawa et al., 2011) of abaxial epidermal pavement cells of 21 DAG first leaves was calculated from a nail polish imprint of cells (about 7 cells each from 10 leaves) midway between the midvein and the lamina edge. The following formula (Minamisawa et al., 2011) was used to calculate the undulation index.

$$\mathrm{UI} = \frac{Ce}{(2 \times \pi) \times \sqrt{Ae/\pi}}$$

Where UI (dimensionless) is the undulation index, Ce (mm) is the cell perimeter, and

Ae (mm^2) is the cell area.

For primary root length and root hair measurements, seedlings were grown vertically in AT media plates and length was measured at 6 DAG. Gravitropic response was measured at 3 hrs after subjecting the vertically grown 4 DAG roots to a 90 degree rotation. Area and perimeter of the leaf epidermal pavement cells and all root measurements were done using NIH ImageJ software. Statistical differences were resolved using Student's t-test and images were processed using Photoshop CS5 (Adobe Inc.).

2.11 Transient transgene expression in Tobacco

Co-transfomation into tobacco was performed at Michigan State University by Dr. Elizabeth Schultz. 35S:GFP:UNH and 35S:SYP61:YFP constructs were electroporated into *A. tumefaciens* strain GV3101 (pMP90). For each construct a transformed colony was inoculated into LB medium supplemented with 100 μg/mL kanamycin, 25 μg/mL gentamycin, and 25 μg/L rifampicin. The resulting cultures were grown at 28-30°C until reaching the stationary phase. Cells were harvested by pelleting 1 mL of culture. Pellets were washed twice with 1 mL of infiltration buffer (50 mM Mes, pH 5.6, 2 mM Na_3PO_4, 0.5% glucose [w/v], and 100 μM acetosyringone [Aldrich]). The washed pellets were first resuspended and then diluted with 1mL of infiltration buffer to give an optical density value of 0.05 for each culture at 600nm. The inoculum was infiltrated into the *N. tabacum* leaves through the stomata of the lower epidermis using a 1-mL needleless syringe. The area of infection was marked

and the plant was left to grow for another 48 hours before analysis by confocal microscopy.

2.12 Confocal microscopy and transient expression analysis

PIN1:GFP (root and first leaves) and PIN2:GFP (roots) expression pattern in *unh-1* and wild type was performed and analysed by confocal microscopy as described previously (Hou et al., 2010). Transient expression of 35S:GFP:UNH and 35S:SYP61:YFP in *N. tabacum* leaves was analysed 48 hrs after infection of the lower epidermis. An upright Leica SP5 laser scanning confocal microscope was used to image the expression pattern (Brandizzi et al., 2002).

2.13 Yeast two-hybrid assay

The yeast two-hybrid screen was performed by using a GALactose metabolism (GAL4) based yeast two-hybrid system (Kohalmi et al., 1997). Full-length coding sequences for *UNH* (pda19438), *VPS52* (pda01753), *VPS53* (pda19355), *VPS54* (pda08404), *VAM3* (pda00856) and *VTI11* (pda02631), were obtained from RIKEN, and *TLG2A* (182L15) and *YPT6* (U83480) were obtained from ABRC. Primer sets, labeled according to the gene name (Table 2.1), were used to amplify *UNH, VPS52, VPS53, VPS54, VTI11, VAM3, TLG2A* and *YPT6*. The amplified product was first ligated into pJET1.2/blunt and then into the bait and/or prey vectors. *UNH* was ligated into the bait vector (pBI770) that expresses GAL4-DNA binding (DB) fusion protein. The other coding sequences were ligated into the prey vector (pBI771) that expresses GAL4-Transcription Activation (TA) fusion protein.

Each construct was transformed as described previously (Gietz and Woods, 2002) into the yeast strain YPB2 (Bartel et al., 1993), grown as described previously (Amberg et al., 2005) and tested for self-activation (activation of reporter genes in absence of a protein interaction). YPB2 allows GAL4-fusion-protein-mediated expression of two reporter genes, *HIS3* (histidine prototrophy) and *LacZ* (β-galactosidase activity). Since none of the proteins showed self-activation, UNH was used as bait for all interactions. Protein-protein interactions between GAL4-DB and GAL-TA fusion proteins were identified by histidine prototrophy in the presence of 3-amino triazole (3-AT, 10 mM) and the expression of *LacZ* using a known interacter (T4) and non-interacter (T7) of *AGAMOUS LIKE4* (*AGL4*) as positive and negative controls, respectively (Kohalmi et al., 1998).

Table 2.1: Primers used for making constructs and genotyping

Primer	Sequence (5'-3')
new10_unhG_F	GCTAGGCGGCCGCCTTCGAGAATGAGAATGCCA
new10_unhG_R	GATCCGCGGCCGCTAATAGAGAGACCCGTG
new5_unh_promo_F	GATCCCCCGGGCTTCGAGAATGAGAATGCCA
new5_unh_promo_R	ATGCCCCGGGTCGCCATTTTTCTAAACTCC
unh_dCAPS_R_BsmAI_F	TGGTTGATATCGAATTTCAAGAGAGTCT
unh_dCAPS_R_BsmAI_R	TGCAGAGGTTGACCCTCATT
UNH_GABI_genespecific	AAGGCCATTTCACAGAAGTTCTTA
UNH_GABI_PCR	ATAATAACGCTGCGGACATCTACATTTT
vam3_4_F	GCCCTTGAAGCTGCAGTTAG
vam3-4_2_R	TCGAAATCAAGCTGCGAGTA
UNH_GFPN_SalI_F	ATGACCGTCGACATGGCGACGGAGGCAGCTCCGATG
UNH_GFPN_STOP_SalI_R	ATGACCGTCGACTTAAGAAGAAACTGTGTTGTTGTT
UNH_Y2H_SalI_F	AGTGCGTCGACAGAAGAAGCAGGAGTTTAGA
UNH_Y2H_NotI_R	ATATAGCGGCCGCGAAGTTACGGTGTAGATTTTACTGG
VPS52_Y2H_SalI_F	AGTGCGTCGACCAACTCTTAATCTCATTAGG
VPS52_Y2H_NotI_R	GATATGCGGCCGCGAGGAACTCTTACTGGTTTGAAAGA
VPS53_Y2H_SalI_F	ATGCAGTCGACTCGAGTGATTTTTGGTTTTATCAT
VPS53_Y2H_NotI_R	GATCAGCGGCCGCGGAAACAAAGGTGGGAATTG
VPS54_Y2H_SalI_F	ATGCAGTCGACGCGCTCTTCTTCATCCAAAA
VPS54_Y2H_NotI_R	GATCAGCGGCCGCGGCGAATAGTCCATCCTCAA
Vam3_Y2H_XmaI_F	TAGTCCCCGGGTCCGATAACCAATTTCTCAATC
Vam3_Y2H_NotI_R	GATAAGCGGCCGCCCAGTCATTGATGCCTTAAGATC
Vti11_Y2H_SalI_F	ATGCAGTCGACCGTTACCTTCTCAGAGTTTTTAG
Vti11_Y2H_NotI_R	GATCAGCGGCCGCCCGTTGTTCTTTGATTTGGTC
TLG2A_Y2H_SalI_F	AGTGCGTCGACAGGGATTTCAAATTTTGACG
TLG2A_Y2H_NotI_R	GATATGCGGCCGCCTTTTCTTATTGATCTAACCAG
YPT6_Y2H_SalI_F	ATGCAGTCGACGAGATCTCGACGTTTCTCAGAT
YPT6_Y2H_NotI_R	GATCAGCGGCCGCGTTGTGTTGTTGTTGCCAAA

The underlined sequences represent the cutting site for restriction enzymes (*SalI, NotI, XmaI* and *BsmAI*) or as denoted in the primer names.
UNH_GABI_genespecific and UNH_GABI_PCR primer sequences were obtained through GABI-kat.

CHAPTER 3: RESULTS

Molecular characterization of *UNHINGED (UNH)* is a continuing project in Dr. Elizabeth Schultz's lab. Previous students have contributed to some of the preliminary data that has formed a basis for my project. I credit the material and results contributed by those students within the text where relevant.

3.1 *unh-1* shows pleiotropic changes to shoot and root characteristics

As the wild type leaf primordium forms, parallel formation of the midvein is in continuation with the central axis of the plant and connects with the vascular tissue of the stem. As the lamina expands, the secondary veins diverge from the midvein and tertiary veins from secondary veins. The secondary veins connect to one another or to higher order veins at the distal margins to form closed areoles (Steynen and Schultz, 2003). An EMS mutagenized *Arabidopsis thaliana* (Col-0 background) population was screened for vein patterning defects (Steynen and Schultz, 2003). A recessive mutant *unhinged-1 (unh-1),* (segregation of 3:1 in F2, χ^2= 0.55 (P>0.54; n=77)), showing a reduction in secondary and tertiary veins as well as a lack of distal vein junctions, was identified.

Comparison of first leaves of wild type 21 DAG (Days After Germination) (Figure 3.1A) and *unh-1* (Figure 3.1B) reveal that *unh-1* leaf veins frequently fail to meet: 33% of the *unh-1* secondary veins (n= 30 leaves) are distally non-meeting compared to 6% of wild type leaves (n=29 leaves) (Cormark, 2006). The number of tertiary veins, quaternary veins and areoles in *unh-1* is also significantly reduced. As

well, the first leaves in *unh-1* are narrower, as indicated by the length/breadth ratio and have more serrations than wild type (Table 3.1). To determine if leaf shape changes were associated with changes to leaf cell size or shape, I measured epidermal pavement cell area and undulation index, a measure of lobes and indentations compared to a perfect circle (Minamisawa et al., 2011). Whereas the average area of *unh-1* epidermal cells is not significantly different from wild type (Figure 3.2E), extremely large and elongated cells are interspersed among the cells of normal size (asterisk in Figure 3.2B), and *unh-1* cells are more undulated (Figures 3.2A, 3.2B and 3.2E).

Like the leaves, *unh-1* cotyledons have a higher number of free ending veins resulting in fewer areoles (Cormack, 2006). As well as the changes to vein pattern, leaf shape and cell dimensions, *unh-1* plants have shorter inflorescence internodes and delayed bolting (Table 3.2, Figure 3.3F). Compared to wild type, *unh-1* primary roots are shorter (Figures 3.3A, 3.3B and 3.3E) but show no significant changes to gravitropic response, density of lateral roots or length of root hairs (Table 3.2). The nature of *unh-1* phenotypic defects including leaf vein pattern, leaf shape and pavement cell dimensions as well as root length are consistent with a global defect to the auxin response or auxin transport pathways.

3.2 Map-based cloning of *UNH*

To determine the molecular nature of *UNH, unh-1* (mutant in Columbia ecotype background) mutant was crossed to *Landsberg erecta* (Landsberg ecotype wild type) and the segregating F2 population was used for molecular mapping.

Narrowing down of the mutation is based on the recombination frequency. The *unh-1* mutation was narrowed to 15 candidate genes between markers 4.11.3 and 4.11.5b on chromosome 4 (Figures 3.4A-3.4C; Cormark, 2006). Sequencing of the candidate genes in the interval revealed a G-to-A substitution in the last nucleotide of the 10th intron of the At4g02030.1 gene (Figure 3.4D; Blackshaw, 2008) suggesting that a splicing defect may account for the phenotype.

I confirmed that the *unh-1* phenotype is the result of mutation in the At4g02030 gene from two sets of experiments. Firstly, the *unh-1* phenotype was rescued by introduction of the wild type At4g02030 gene (pUNH) (compare Figures 3.1B and 3.1C). Secondly, a GABI-Kat T-DNA insertion line (GABI_KAT520G08) with an insertion in the 7th intron of AT4g02030 (Figure 3.4D) has significantly reduced tertiary and quaternary veins compared to wild type (Figure 3.1D, Table 3.1). F1 plants following a cross of the Gabikat line to *unh-1* had a reduced vein complexity and narrower leaves than wild type (Figure 3.1E, Table 3.1), indicating that the *unh-1* mutation and the Gabikat insertion are alleles of the same gene, At4g02030. The Gabikat line is designated *unh-2.*

3.3 *UNH* is a member of the plant GARP complex

At4G02030/UNH is predicted to encode a VPS51 domain at its N-terminal (Marchler-Bauer et al., 2011). The VPS51 protein is one of the four subunits of the GARP complex. UNH contains a well-conserved motif, LVYENYKFISATDT, (Figure 3.5) found in the VPS51 domain of higher eukaryotes (Luo et al., 2011). Two other genes in *Arabidopsis*, At1g10385 and At5g16300, are also predicted to encode

proteins with VPS51 domains but have considerably less conservation of the motif (Figure 3.5). Mutations in genes encoding three subunits (VPS52, VPS53, VPS54) of the *Arabidopsis* GARP complex have been identified and characterized (Guermonprez et al., 2008; Wang et al., 2011). Insertional mutations in these genes are homozygous lethal and no phenotype similar to *unh-1* has been reported. The poky pollen tube (*pok*) mutant resulting from a T-DNA insertion in the *VPS52* gene has a short pollen tube phenotype (Lobstein et al., 2004). Similarly, insertions in VPS53 and VPS54 coding genes show male transmission defects and *heat-intolerant1-1 (hit1-1)*, a nonsense mutation in *VPS53/HIT1,* shows defects to heat tolerance (Guermonprez et al., 2008; Wang et al., 2011).

To determine if UNH forms a part of the GARP complex, I performed yeast two-hybrid assays and tested for interactions between UNH and VPS52, VPS53 or VPS54. Yeast two-hybrid is used to detect protein interaction of 'bait' fused to DNA Binding (DB) domain with 'prey' fused to Transcription Activation (TA) domain (Kohalmi et al 1998). Interaction of bait and prey brings together the two interacting domains and initiates the transcription of two reporter genes; the *HIS3* gene that allows the growth of cells in media lacking histidine (His-) and the *LacZ* gene that encodes the enzyme β-galactosidase allowing the cleavage of the substrate X-gal. When X-gal is cleaved, a blue color is observed. The pBI770 plasmid (prototroph for leucine) was used to express UNH (VPS51) as GAL4-DB (bait) and the pBI771 plasmid (prototroph for tryptophan) to express VPS52, VPS53 or VPS54 as GAL4-TA (prey) (Kohalmi et al., 1997). Growth in media lacking His and synthesis of β-galactosidase (LacZ) were used as controls (Figure 3.6A). None of the bait and prey

constructs showed self-activation (UNH-DB and VPS52-TA shown in Figure 3.6B). My analysis for interaction showed that UNH/VPS51 interacts with VPS52 (Figure 3.6C) suggesting that UNH/VPS51 is a member of the plant GARP complex. UNH however did not show interactions with VPS53 and VPS54 (Figure 3.6C).

While GARP tethering factors provide specificity to the transport vesicles, the SNAREs mediate the fusion of the vesicle with the target membrane and small GTPases regulate multiple events during the process (Whyte and Munro, 2002). The GARP complex, through interaction with Yeast Protein Transport-6 (YPT6), a member of Rab-GTPase family, is recruited to the TGN (Conibear and Stevens, 2000; Siniossoglou and Pelham, 2001). I tested for interaction of UNH with YPT6 and the result was negative (Figure 3.6C). A possibility is that YPT6 specifically interact with other members of the GARP complex in *Arabidopsis* to recruit the complex to the TGN during the vesicle fusion event.

In yeast and humans, VPS51 and ANG2 (VPS51 orthologue in human) are known to interact with the t-SNAREs TLG1p and Syntaxin 6 (TLG1 orthologue in mammals) respectively (Pérez-Victoria et al., 2010b). When I tested for interaction of UNH with TLG2A, the homologue of which in yeast is known to interact with TLG1, the results was negative (Figure 3.6C).

The TLG1 homologue in plants is SYP61. SYP61 is a member of SYP41 complex, one of the 10 complexes of SYntaxin of Plants (SYP) gene families (Sanderfoot et al., 2000). The SYP41 complex includes VPS41, VPS61, VTI12 and other regulatory proteins such as VPS45 (Bassham et al., 2000; Bryant and James, 2001; Sanderfoot et al., 2000).

Proteins that interact are expected to be a part of the complex and/or colocalize in the same organelle/membrane. To determine the subcellular localization of UNH, I generated the 35S:GFP:UNH fusion construct and Dr. Elizabeth Schultz co-expressed it with SYP61:YFP (Figure 3.7), which localizes to the TGN as well as to the PVC (Bassham et al., 2000; Bryant and James, 2001; Sanderfoot et al., 2000; Sanderfoot et al., 2001) in tobacco epidermal cells. Transient coexpression in tobacco epidermal cells is a fast and convenient method of assaying the colocalization of two or more proteins. I was able to detect that UNH colocalizes partially with SYP61 (arrows in Figure 3.7C) suggesting that at least a portion of the UNH proteins are localized at the TGN and/or PVC. Individual punctae of 35S:GFP:UNH as well as 35S:SYP61:YFP that did not colocalize (arrowheads in Figure 3.7C) are also present. The partial co-localization of 35S:SYP61:YFP and 35S:GFP:UNH suggests that as in yeast and mammals, UNH interacts with SYP61.

C. elegans VPS51 interacts with the early, late and Golgi-endosome interface associated SNAREs (Luo et al., 2011). While no mutations to Golgi associated SNAREs in *Arabidopsis* have been reported to have phenotypes similar to *unh-1*, mutations in *VAM3/SYP22,* whose product is a member of the vacuolar membrane localized t-SNARE super family, shows vein pattern defects very similar to *unh-1* (Shirakawa et al., 2009) (Table 3.1, Figure 3.1F). As well, the adult *vam3-4* shoot is much shorter than wild type (Ohtomo et al., 2005). An interacting partner for VAM3, VTI11, is expressed in the PVC and is a member of the v-SNARE family. *vti11* mutant show agravitropic shoots (Kato et al., 2002). The first leaves of *vti11* mutants do not have a leaf vein phenotype (Table 3.1, Figure 3.1H) but enhance *vam3-4* defects

(Shirakawa et al., 2009). To see if UNH interacts with these SNARES, yeast two-hybrid interaction assays were performed with UNH (VPS 51) as bait and VAM3 or VTI11 as preys. The results show that UNH does not interact with VAM3 or VTI11 (Figure 3.6C) suggesting that it acts at a different step. To further test this idea, I generated double mutants amongst the gene pairs. Consistent with independent action of the genes in different steps of the same pathway, both *unh-1 vam3-4* and *unh-1 vti11* show an additive phenotype more extreme than either single mutant with respect to leaf veins (Table 3.1, Figures 3.1G and 3.1I) and shoot phenotype (Figure 3.3F).

3.4 *UNH* is expressed in both root and shoot

The phenotypic changes together with the changes to *DR5:GUS* expression in roots and shoots of *unh-1* mutants (Cormark, 2006) suggest that *UNH* acts throughout plant development. Expression of a genomic region including the coding region and a 5KB upstream region is sufficient to complement the *unh-1* phenotype, suggesting that the 5KB region is sufficient to confer the endogenous expression pattern. To assess the expression of *UNH*, I fused the 5KB upstream region to the β-glucuronidase (*GUS*) reporter gene (*pBIUNH:GUS*) and analyzed *GUS* expression in transformed wild type plants. *pBIUNH:GUS* is expressed in both root and shoot of young seedlings (Figure 3.8A). In roots, the expression is throughout the epidermis within the elongation and differentiating zones and in the emerging lateral roots (Figures 3.8B and 3.8C). In immature flowers (Figure 3.8E), *pBIUNH:GUS* is slightly

expressed in the veins of petals (Figure 3.8F) and is expressed in pollen grains (Figure 3.8G).

In first leaves, *pBIUNH:GUS* expression begins weakly and diffusely at 2 DAG (Figure 3.8H). By 3 DAG, the expression is strong in several cell files surrounding the presumptive secondary veins (Figure 3.8I). Also at 3 DAG and 4 DAG, *pBIUNH:GUS* is expressed in the leaf margin adjacent to the position where the next set of secondary veins will form (arrowheads in Figure 3.8I and 3.10J). Expression of *pBIUNH:GUS* progressively narrows as veins form (Figure 3.8K). This narrowing of expression is similar to that shown for *FKD1:GUS*. FKD1 is proposed to respond to auxin and hence be a component of the auxin canalization regulatory loop (Hou et al., 2010). Like *FKD1*, *UNH* contains an ARF binding motif in its 5' upstream region of transcriptional start site. To test the auxin responsiveness of *UNH,* I treated *pBIUNH:GUS* seedlings with 2,4-D and compared expression in roots at 2 DAG. Treatment with auxin transport inhibitor NPA or synthetic auxin is known to shift the expression of auxin responsive markers (Sabatini et al., 1999). Compared to untreated roots, *pBIUNH:GUS* expression following 2,4-D treatment is more focused and shifted towards the apex (Figure 3.8D) suggesting that *UNH* is auxin responsive.

3.5 Marginal PIN1:GFP expression is expanded in *unh-1* leaves

The known role of the GARP complex in retrograde vesicle cycling within yeast and metozoans combined with the auxin related defects in *unh* mutants suggest that *unh* may be defective in PIN localization. To assess if PIN is mislocalized in *unh-1* plants, I introduced PIN1:GFP and PIN2:GFP into *unh-1* and assessed their

localization in both roots and leaves. Within roots, PIN2:GFP is expressed apically in epidermal cells and basally on cortical cells, whereas PIN1:GFP is expressed basally within the stele (Vieten et al., 2005). Their expression thus overlaps with UNH based on the *pBIUNH:GUS* expression pattern in the root tip (compare Figure 3.8C to Figure 3.9A, 3.9C). When I compared localization of PIN1:GFP and PIN2:GFP in roots of wild type and *unh-1*, no differences were obvious (Figure 3.9).

I next examined the PIN1:GFP expression in developing leaves. Consistent with the delay in formation of *DR5:GUS* apical auxin maxima (Cormark, 2006), *unh-1* is delayed by a half day with respect to midvein PIN1 Expressing Domains (PED) (compare Figures 3.10A and 3.10F). To allow comparison between equivalent developmental stages, I quantified the developmental stages of the first leaf primordium by analyzing primordial length and the number of PED in presumptive secondary and tertiary veins (Table 3.3). Based on these observations and the overall reduction in the secondary and tertiary vein number in *unh-1*, I consider 2.5 DAG, 3 DAG and 4 DAG wild type to be at an equivalent developmental stage as 3 DAG, 4 DAG and 5 DAG *unh-1* respectively.

As might be expected from the normal midvein in *unh-1* leaves, early PIN1:GFP expression in *unh-1* was indistinguishable from wild type with respect to asymmetric localization on the apical side of the epidermal cells (arrows in Figure 3.10A and 3.10F), formation of apical maxima, and localization within the subepidermal cells along the future midvein vasculature (Figures 3.10A and 10F). Concurrent with its expression in the midvein, the PIN1:GFP expression at the apical epidermal cells is reduced and new zones of expression appear at the lateral leaf

margins. Using a LUT saturation index as an indication of strong PIN1:GFP expression, I compared the number of cells showing strong lateral expression of PIN1:GFP and their association with the PEDs of secondary veins.

In 2.5 DAG wild type, about 4 cells of the lateral margin show strong PIN1:GFP expression (marginal PED) associated with generation of the first secondary vein PED (Table 3.3, asterisks in Figure 3.10B). In *unh-1*, at a corresponding stage (3 DAG), the marginal PED associated with first secondary vein PED is larger, with about 7 cells showing strong expression (Table 3.3, asterisks in Figure 3.10G). At 3 DAG wild type, the marginal PED shifts proximally, includes six cells and is associated with the second secondary vein PED (Table 3.3, figure 3.10C). In a corresponding *unh-1* (4 DAG) the marginal PED associated with the second secondary vein PED includes 9 cells (Table 3.3, Figure 3.10H). In 4 DAG wild type, marginal PED again shifts proximally, includes about 7 cells, and is associated with the third set of secondary veins (Table 3.3, asterisks in Figures 3.10D and 3.10E). Comparatively in a 5 DAG *unh-1* leaf the marginal PED includes about 13 cells (Table 3.3, asterisks in Figures 3.10I and 3.10J). From these results I conclude that marginal expression shows appropriate positional changes and is properly associated with secondary vein formation. However each marginal PED is expanded in *unh-1* compared to wild type.

3.6 PIN:GFP and *ATHB8:GUS* expression pattern is altered in *unh-1* secondary veins

unh-1 shows defects to serrations and has fewer secondary veins that rarely meet distally (Table 3.1, Figure 3.1B). The regions of auxin maxima at the leaf margins are proposed to regulate both serrations and the generation of secondary veins in leaves (Bilsborough et al., 2011; Scarpella et al., 2010). I asked if the defects to PIN1:GFP expression at the margins were correlated with changes to PIN1:GFP expression in the secondary veins. My spatio-temporal analysis suggests that PIN1:GFP expression and localization in a wide zone surrounding the LLD is indistinguishable between wild type and *unh-1* at 2.5 DAG and 3 DAG respectively, (Figures 3.10B and 3.10G). In both wild type and *unh-1*, the expression of LLD narrows down towards the proximal midvein PED. The expression of PIN1 follows in the ULD, which extends distally to join the secondary vein PED strand with the midvein. In 3 DAG wild type, a loop of PIN1 expression predicting the first set of secondary veins is complete and expression within LLD of the second set of secondary veins is initiated (Figure 3.10C). While there is no noticeable difference to the LLD formation at an equivalent developmental stage of *unh-1* (4 DAG) (Figure 3.10H), the formation of ULD does not occur and cells with apical localization of PIN1:GFP are absent (arrowhead in Figure 3.10H). The lack of the ULD persists in further sets of secondary veins (arrowheads in Figure 3.10I).

The lack of PIN1:GFP in the distal loop (ULD) of the secondary veins may suggest that the cells are not being recruited to a procambial fate. To test this idea I used *ATHB8:GUS* reporter gene expression analysis. I compared wild type

ATHB8:GUS expression with *unh-1 ATHB8:GUS* expression in the developing first leaves. *ATHB8*, an auxin responsive homeobox gene, encodes a member of the HD-Zip class III transcriptional factors (Baima et al., 1995; Kang and Dengler, 2002; Scarpella et al., 2004). Early expression of *ATHB8:GUS* coincides with the development of procambium (Scarpella et al., 2006; Figures 3.11A and 3.11C). Consistent with the delay in DR5:GUS expression (Cormark, 2006) as well as pattern of PIN1:GFP expression, *ATHB8:GUS* expression is delayed and does not form complete loops in *unh-1* (arrows in Figures 3.11D and 3.11F).

3.7 The *unh-1* phenotype is suppressed by *pin1, pin2* and *aux1* mutation

I reasoned that if the *unh-1* leaf phenotype was the result of expanded PIN1 expression in the leaf margin, it might be rescued by mutation to PIN1. The *pin1-1* mutant has a leaf phenotype not significantly different from wild type except a more rounded leaf shape (Table 3.1, Figure 3.1J). Consistent with my prediction, *pin1-1* suppressed all aspects of the *unh-1* leaf phenotypes: leaf shape, epidermal cell shape (UI) and vein pattern phenotype, resulting in a leaf that was indistinguishable from wild type for every character except that it had increased numbers of secondary veins (Table 3.1, Figures 3.1K, 3.2A-3.2E).

The generation of auxin maxima in the leaf epidermis depends not only on auxin efflux but also on the influx activity (Reinhardt et al., 2003). It has been proposed that AUX1, an auxin influx protein, expressed on the abaxial epidermis of leaf primordia, maintains auxin in the margin. This scenario suggests that AUX1 acts with PIN1 in maintaining marginal auxin and further that reduction to AUX1 activity

might relieve the effects of ectopic PIN1 in the *unh-1* leaf margin. To test this idea I analyzed 21 DAG first leaf vein phenotype of *unh-1 aux1-7* double mutant and compared it with the wild type. Plants with *aux1-7* mutation alone have leaves that are rounder and have simpler vein pattern compared to wild type (Table 3.1, Figure 3.1L). Introduction of *aux1-7* into *unh-1* results in a less severe *unh-1* phenotype: the leaves are wider with fewer serrations and have a more complex phenotype with more vein meetings (Table 3.1, Figure 3.1M). The complete suppression of *unh-1* leaf phenotype by *pin1-1* and its partial suppression by *aux1-7* strongly supports the idea that the *unh-1* phenotype results from extended marginal PIN1 expression causing increased auxin within the leaf margin.

Reduced level of *DR5:GUS* expression in the root apex (Cormack, 2006) combined with the shorter root length of *unh-1* suggest that *unh-1* roots have reduced auxin levels possibly resulting from increased levels of PIN2 in the elongation zone. To test the idea that reducing the level of PIN2 in the root might relieve the *unh-1* root length phenotype, I compared the the root length between WT, *unh-1*, *eir1-1* and *unh-1 eir1-1* double mutant (Cormark, 2006). EIR/PIN2 is a root specific efflux protein; the *pin2/eir1-1* mutant roots are agravitropic and have a reduced sensitivity to ethylene (Lusching et al., 1998). Introduction of *eir1-1* suppressed the *unh-1* root phenotype (Figures 3.3C-3.3E), suggesting that the short *unh-1* roots are due to ectopic *PIN2*.

Table 3.1: Leaf vein pattern and leaf shape characteristics of 21 DAG first leaves for various genotypes

Genotypes	Secondaries	NMS	Tertiaries	Quaternaries
Wild type (29)	8.8 ± 1.5	0.4 ± 0.7	22.4 ± 4.3	4.9 ± 2.1
unh-1 (30)	6.2 ± 1.2 [a]	3.1 ± 1.3 [a]	6.6 ± 3.0 [a]	0.9 ± 0.9 [a]
unh-2 (19)	8.3 ± 1.1 [b]	0.8 ± 0.6 [b]	15.2 ± 3.2 [ab]	2.6 ± 1.2 [ab]
unh-1 X *unh-2* F1 (21)	8.4 ± 0.9 [b]	0.8 ± 0.7 [b]	15.9 ± 5.2 [ab]	2.3 ± 1.6 [ab]
vam3-4 (16)	6.7 ± 1.2 [a]	1.8 ± 1.2 [ab]	4.8 ± 2.5 [ab]	0.6 ± 0.6 [a]
unh-1 vam3-4 (21)	3.9 ± 0.8 [abc]	3.0 ± 1.1 [ac]	0.3 ± 0.6 [abc]	0 [abc]
vti11 (18)	9.2 ± 0.6 [b]	0.8 ± 0.8 [b]	21.0 ± 4.1 [b]	3.9 ± 1.9 [b]
unh vti11 (22)	6.3 ± 0.9 [ac]	4.5 ± 1.4 [abc]	4.7 ± 2.0 [abc]	0.3 ± 0.5 [abc]
pin1 (19)	9.1 ± 1.7 [b]	0.5 ± 0.8 [b]	23.6 ± 4.0 [b]	3.6 ± 4.0 [b]
unh-1 pin1-1 (23)	11.5 ± 2.7 [abc]	0.7 ± 0.8 [b]	21.3 ± 9.4 [b]	1.7 ± 1.8 [a]
aux1-7 (31)	8.2 ± 1.3 [b]	0.5 ± 0.6 [b]	17.3 ± 5.8 [ab]	2.5 ± 1.7 [ab]
unh-1 aux1-7 (37)	8.0 ± 1.3 [ab]	1.8 ± 1.2 [abc]	10.3 ± 4.4 [abc]	0.5 ± 0.7 [abc]

Genotypes	Areoles	L/B	Serrations
Wild type (29)	22.0 ± 4.7	1.3 ± 0.1	0.1 ± 0.3
unh-1 (30)	4.5 ± 2.3 [a]	1.7 ± 0.2 [a]	0.7 ± 0.8 [a]
unh-2 (19)	15.6 ± 4.1 [ab]	1.4 ± 0.1 [b]	0.1 ± 0.3 [b]
unh-1 X *unh-2* F1 (21)	15.9 ± 4.8 [ab]	1.4 ± 0.1 [ab]	0.2 ± 0.5 [b]
vam3-4 (16)	6.1 ± 1.7 [ab]	1.5 ± 0.1 [ab]	0.4 ± 0.6
unh-1 vam3-4 (21)	1.0 ± 1.1 [ab]	2.2 ± 0.9 [abc]	0.4 ± 0.7
vti11 (18)	20.8 ± 4.1 [b]	1.4 ± 0.1 [b]	0.1 ± 0.3 [b]
unh vti11 (22)	2.1 ± 1.1 [abc]	1.7 ± 0.2 [ac]	0.5 ± 0.7 [ac]
pin1 (19)	23.0 ± 6.2 [b]	1.1 ± 0.1 [ac]	0 [b]
unh-1 pin1-1 (23)	19.0 ± 8.7 [b]	1.4 ± 0.2 [bc]	0.1 ± 0.3 [b]
aux1-7 (31)	17.0 ± 5.5 [ab]	1.2 ± 0.1 [ab]	0.1 ± 0.3
unh-1 aux1-7 (37)	8.1 ± 2.4 [abc]	1.4 ± 0.1 [abc]	0.3 ± 0.7 [b]

Values represent mean ± standard deviation. Number in parentheses represents numbers of leaves scored. Abbreviations for phenotypic characters: Non-Meeting Secondaries (NMS), Leaf length:breadth ratio (L/B)

[a] significantly different from wild type ($p<0.05$).

[b] significantly different from *unh-1* ($p<0.05$).

[c] double mutant is significantly different from its respective non-*unh-1* single mutant ($p<0.05$)

Table 3.2: Comparison of phenotypic characters between wild type and *unh-1*

Genotypes	Days to bolting of 50% of plants	Gravitropic response in 3 hrs [b]	Lateral root density (per mm) [c]	Root hair length (mm)	Internode length (mm)
Wild type	15 (21)	40.0 ± 18.2 (39)	0.3 ± 0.1 (18)	0.6 ± 0.1 (166)	14.4 ± 0.04 (21)
unh-1	18 (16) [a]	38.5 ± 14.1 (38)	0.3 ± 0.2 (17)	0.6 ± 0.1 (134)	12.9 ± 0.04 (16)

Values represent mean ± standard deviation. Number in parentheses represents sample size

[a] = significantly different from wild type ($p<0.05$)

[b] = bending away (in degrees) from the vertical axis after a 90 degrees rotation.

[c] = Number of emerging lateral roots were counted on vertically grown 6DAG roots.

Table 3.3: PIN1:GFP expression in early leaf veins and margins

Geno-types	Number of secondary vein PED	Number of tertiary vein PED	Number of cells in marginal PED	Primordium length (μm)
WT 2.5 DAG	0.7 ± 0.4 (23)	0 (23)	3.9 ± 0.9 (15)	108.8 ± 9.4 (23)
WT 3 DAG	3.2 ± 1.6 (20)	0.7 ± 1.3 (20)	6.3 ± 1.5 (42)	144.5 ± 23.0 (30)
WT 4 DAG	5.9 ± 1.5 (20)	1.8 ± 1.4 (20)	7.04 ± 3.0(67)	352.7 ± 75.7 (15)
WT 5 DAG	ND	ND	6.0 ± 1.6	490.8 ± 63.2
unh-1 3 DAG	0.9 ± 1.1 (37) [b]	0 (37)	6.8 ± 1.4 (39) [a]	114.4 ± 17.2 (25) [b]
unh-1 4 DAG	2.4 ± 0.8 (21) [b]	0 (21) [ab]	9.2 ± 3.3 (49) [ab]	185.8 ± 19.9 (15) [ab]
unh-1 5 DAG	3.5 ± 0.8 (14) [a]	0.1 ± 0.5 (14) [a]	12.8 ±3.8 (38) [ab]	438.1 ± 49.5 (15) [ab]

Values represent mean ± standard deviation. Number in parentheses represents sample size.

Abbreviations used: PED: PIN1:GFP expression domain (showing strong Lateral Expression), ND: Not Determined; PIN1:GFP expression was rarely visible in distal secondary veins and tertiary veins in wild type 5 DAG first leaves.

[a] significantly different from wild type at the same stage of development ($p<0.05$).

[b] significantly different from wild type at the same day after germination ($p<0.05$).

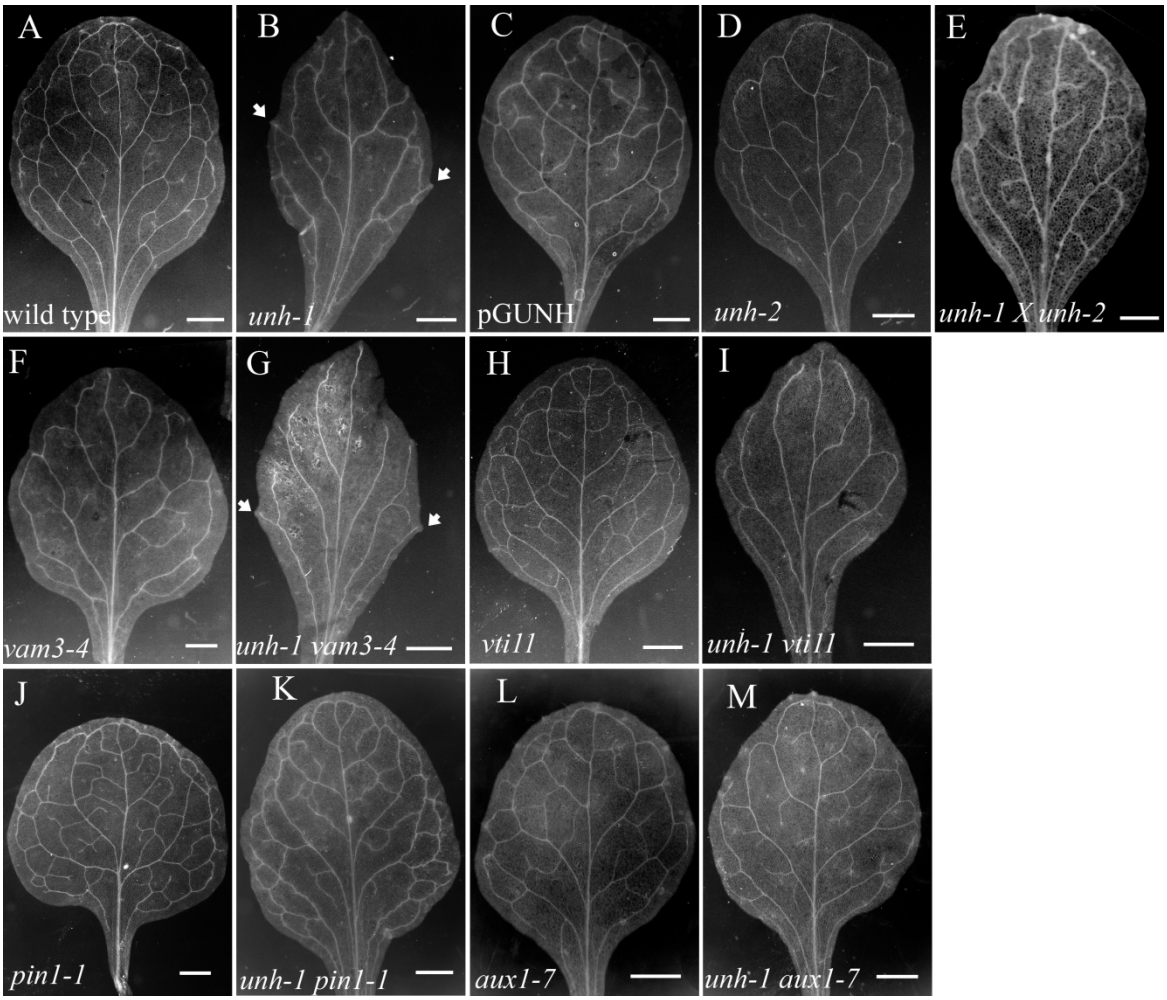

Figure 3.1: First leaf vein phenotype of various genotypes at 21 DAG.
Leaf vein phenotype of wild type (A), *unh-1* (B), *unh-1* transformed with pGUNH (C), *unh-2* (D), *unh-1* X *unh-2* F1 (E), *vam3-4* (F), *unh-1 vam3-4* (G), *vti11* (H), *unh-1 vti11* (I), *pin1-1* (J), *unh-1 pin1-1* (K), *aux1-7* (L), *unh-1 aux1-7* (M). Arrows in B and G indicate serrations in *unh-1* and *unh-1 vam3-4* respectively. Scale bars = 1 mm.

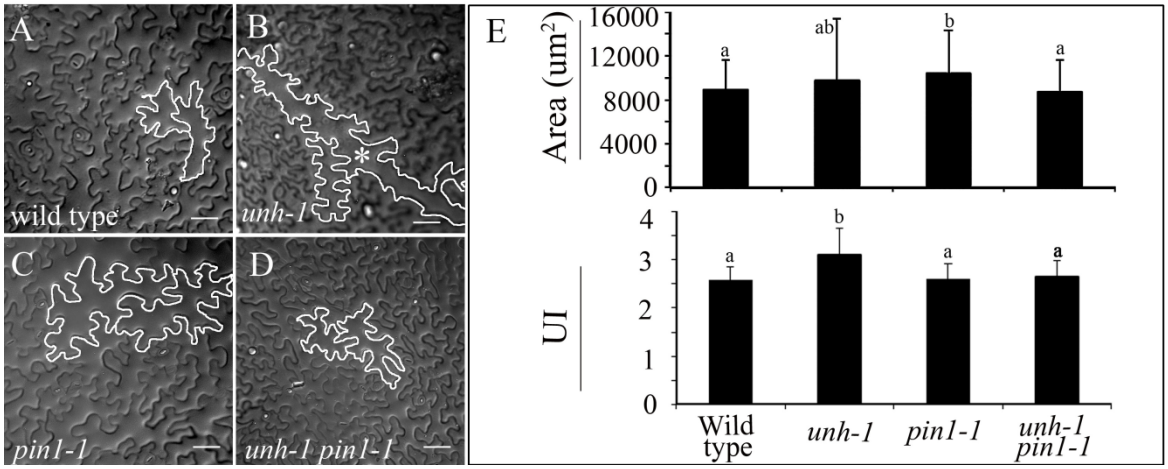

Figure 3.2: Epidermal cell phenotype of various genotypes
(A) to (D) abaxial epidermal cells of wild type (A), *unh-1* (B), *pin1-1* (C), *unh-1 pin1-1* (D). Scale bars = 50 μm. Asterisk in B indicates one of the large cells interspread in *unh-1* leaf epidermis. (E) Graphs representing the area and undulation index (UI) of the abaxial epidermal cells. Error bars represent SD, ^{b} is significantly different from ^{a} ($p<0.05$). Sample sizes are wild type (n=70), *unh-1* (n=62), *pin1-1* (n=70), *unh-1 pin1-1* (n=70).

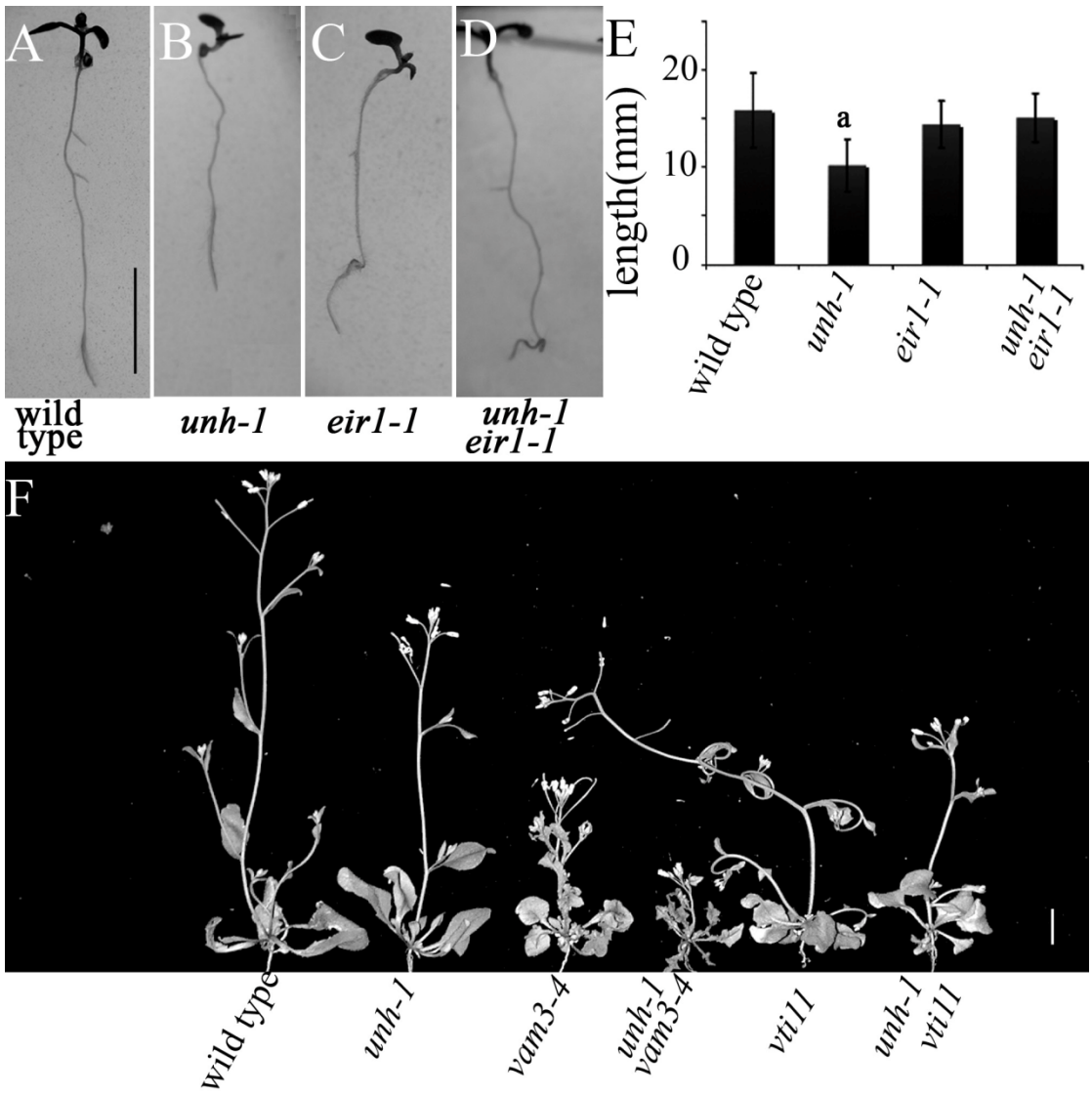

Figure 3.3: Seedling and adult plant phenotypes of various genotypes.
(A to D) 6 DAG seedling of wild type (A), *unh-1* (B), *eir1-1* (C) *unh-1 eir1-1* (D) grown vertically on AT media plates. Scale bars = 5 mm.(E) Graph comparing root length among different genotypes . a = significantly different from the other genotypes. Sample sizes are wild type (n=24) *unh-1* (n=25), *eir1-1* (n=26), *unh-1 eir1-1* (n=28). (F) 26 DAG plants of various genotypes grown on soil. Scale bar = 1 cm.

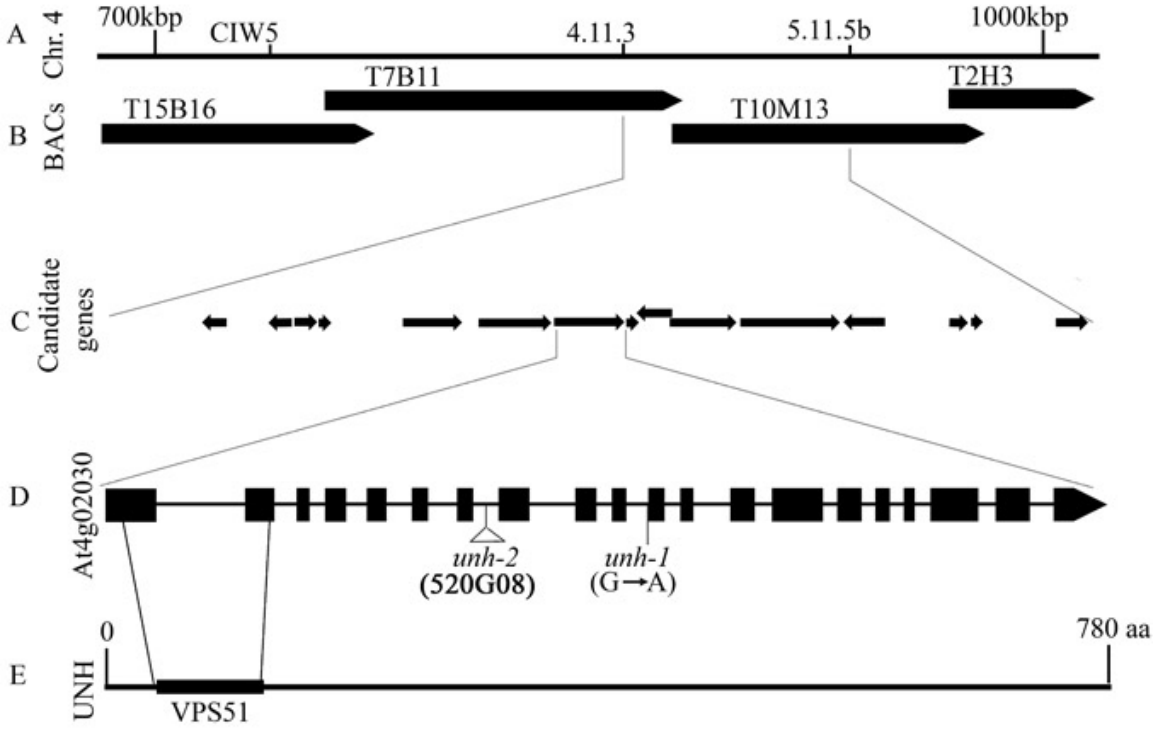

Figure 3.4: Positional cloning of *UNH*.
Recombination analyses determined that markers 4.11.3 and 5.11.5b flanked *UNH* in chromosome 4 (A) a region contained in the Bacterial Artificial Chromosomes (BACs) T7B11 and T10M13 (B). The zone contains 15 candidate protein coding genes (C). Transcribed region of At4g02030.1 showing exons (blocks) and introns (connecting lines). Position of *UNH* alleles, *unh-1* (G->A substitution) and *unh-2* (T-DNA insertion) (D). The 780 amino acid sequence of UNH showing the N-terminal VPS51 domain (E).

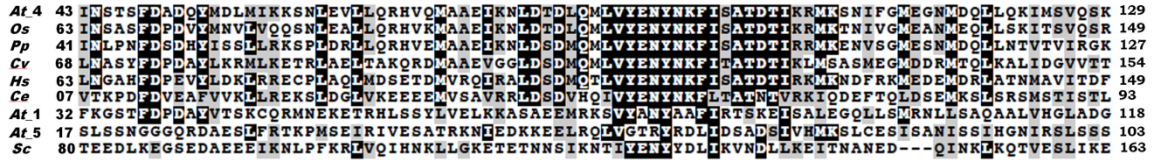

Figure 3.5: Multiple sequence alignment of VPS51 orthologues from representative eukaryotes.

Multiple sequence alignment of the VPS51 domain sequence (N-terminal 87 amino acid sequence of At4g02030.1) with putative VPS51 orthologues. Minimal conserved protein domain described for the yeast VPS51 was used as a cutoff for sequence alignment. CLUSTAL W and BOXSHADE were used to perform alignment and shading respectively. Identical and conserved sequences are represented by black and grey shades respectively. Numbers represent start and end of the amino acid sequence used for each protein encoded by the genes: *At_4 = Arabidopsis thaliana* (At4g02030), *Os = Oryza sativa, Pp = Physcomitrella patens, Cv = Chlorella variabilis, Hs = Homo sapiens, Ce = Caenorhabditis elegans, At_1 = Arabidopsis thaliana* (At1g10385), *At_5 = Arabidopsis thaliana* (At5g16300), *Sc = Saccharomyces cerevisiae*.

Amino acid sequence data used for the alignment can be found in NCBI GenBank/EMBL under the following accession numbers: *Arabidopsis thaliana* UNH/VPS51 (AEE82113.1), *Arabidopsis thaliana* At1g10385/VPS51 (AEE28573.1), *Arabidopsis thaliana,* At5g16300/VPS51 (AED92277.1), *Oryza sativa* OSJNBb0016H12.27 (AAP03421.1), *Saccharomyces cerevisiae* VPS 51/ YKR020W (AAS56882.1), *Physcomitrella patens* subsp. *patens* PHYPADRAFT_188366 (EDQ65333), *Chlorella variabilis* CHLNCDRAFT_138739 (EFN52716.1), *Homo sapiens* ANG2 /C11orf2 (AAF21627), *Caenorhabditis elegans* B0414.8 (NP_001020972.1)

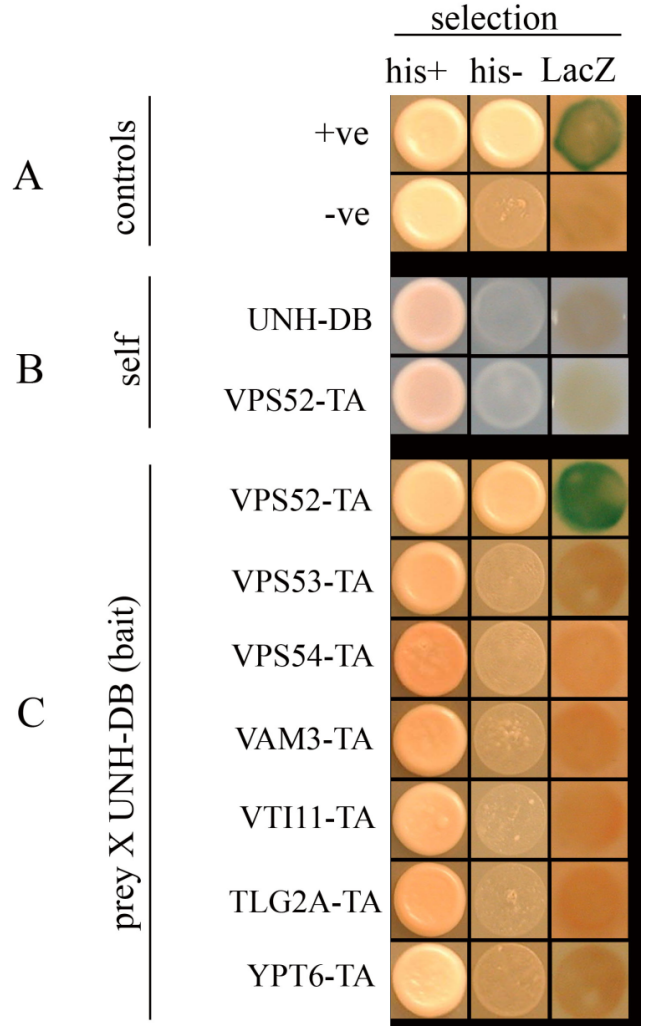

Figure 3.6: Yeast two-hybrid assays for interaction of UNH

Yeast two-hybrid assays for interaction of UNH with *Arabidopsis* VPS52, VPS53, VPS54, VAM3, VTI11, TLG2A and YPT6.

(A) Growth of positive control (AGL4 interacter) on His plate and production of LacZ were used to confirm the interactions. AGL4 non-interacter was used as a negative control. (B) No self activation was seen for UNH- GAL4-DB (bait) and VPS52-GAL4-TA (prey). (C) Assays for interaction of UNH-BD with GARP complex subunits (VPS52, VPS53, VPS54, SNAREs (VAM3, VTI11, TLG2A), or GTPase (YPT6) in prey (GAL4-TA). his+: Growth of yeast on media without leucine and/or tryptophan for bait and/or prey selection respectively; his-: testing for histidine prototrophy on media lacking leucine, tryptophan, histidine and supplemented with 10 µM 3-AT; lacZ: yeast tested for β-galactosidase activity (for 2 hours). Transformation of bait or prey constructs alone tests for self-activation while double transformations test for protein interactions.

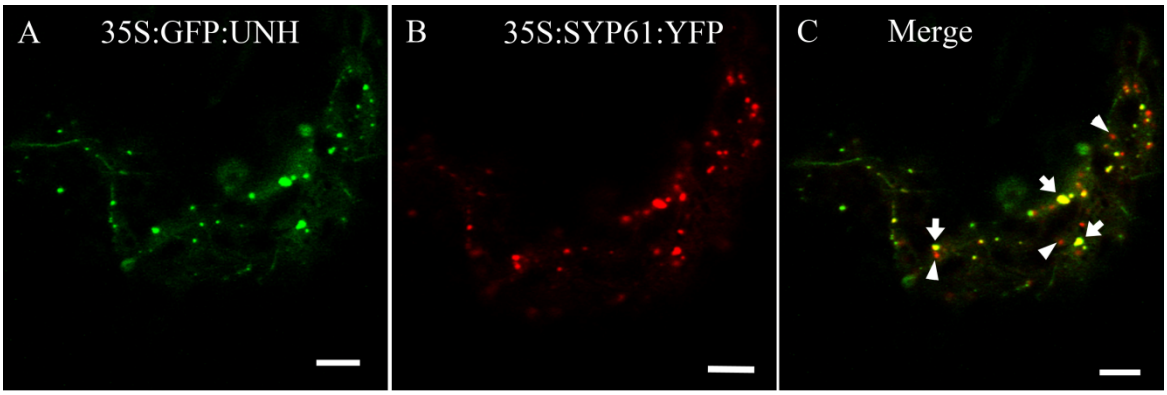

Figure 3.7: Subcellular localization of 35S:GFP:UNH and 35S:SYP61:YFP in tobacco epidermal cells

Confocal images of *Nicotiana tabacum* leaf epidermal cells transiently expressing 35S:GFP:UNH (A), 35S:SYP61:YFP (B) and merged images of A and B (C). 35S:GFP:UNH and 35S:SYP61:YFP colocalized at punctate structure (white arrows). Both proteins are also localized to additional structures (white arrowheads). Scale Bar: 5 µm

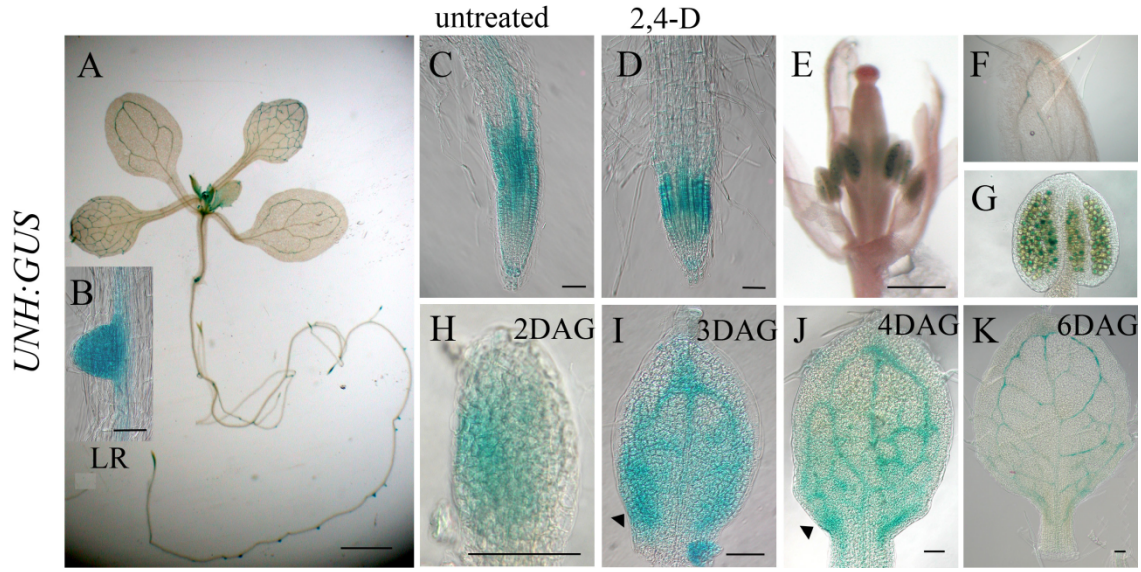

Figure 3.8: *UNH:GUS* expression in various organs of wild type *Arabidopsis* *UNH:GUS* expression in wild type seedling (A), lateral root (B), primary root (C-D), floral bud (E), petal (F), anther (G) and developing first leaves (H-K). Arrowheads indicate leaf marginal expression. Scale bar = 2 mm (A), 1mm (E), 50 μm (all others). Stained for 18 hours, viewed with dissection microscope (A, E) and differential interference contrast (all others).

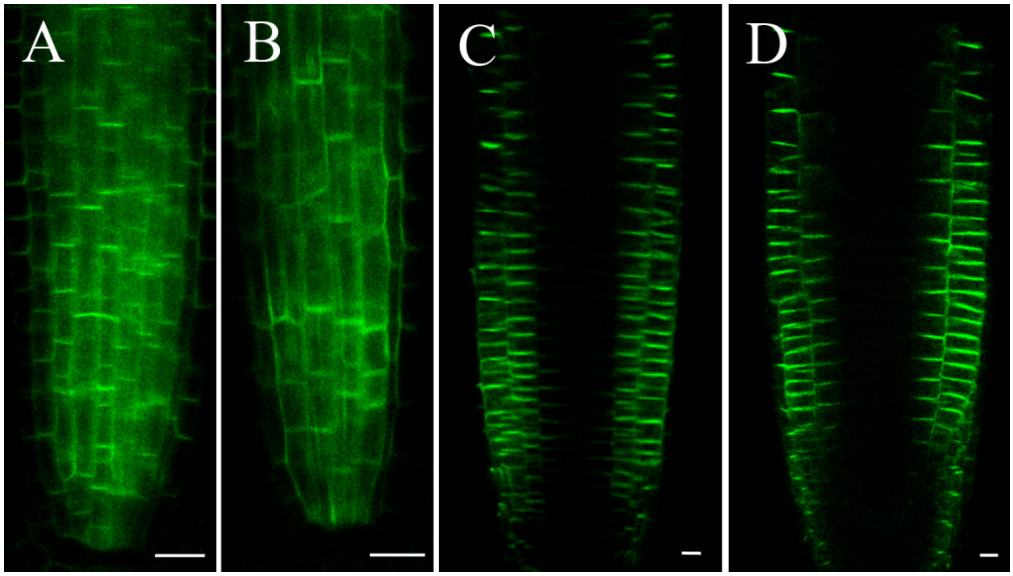

Figure 3.9: PIN1:GFP and PIN2:GFP expression in *Arabidopsis* root
PIN1:GFP (A, B) at 2.5 DAG and PIN2:GFP (C, D) at 4 DAG of wild type (A, C) and *unh*-1 (B, D) as viewed under confocal microscopy. Scale bars = 10μm

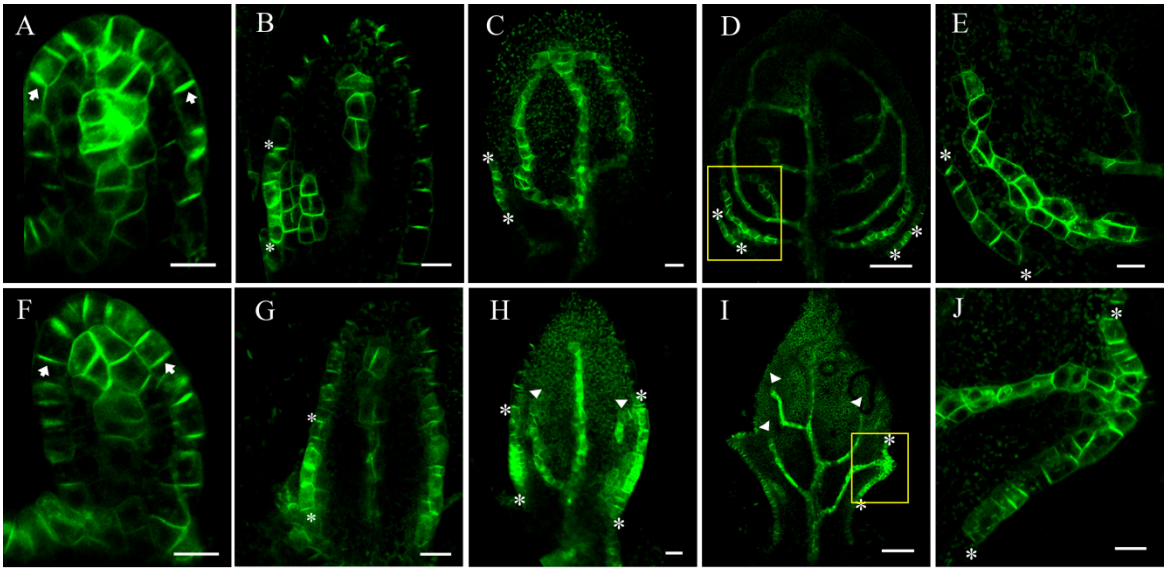

Figure 3.10: PIN1:GFP expression in early developing first leaf of *Arabidopsis* PIN1:GFP expression in wild type (A-E) and *unh-1* (F-J) first leaf primordia at 2 DAG (A) 2.5 DAG (B,F), 3 DAG (C,G), 4 DAG (D,E,H), 5 DAG (I,J). Images in E and J are enlarged portion of boxes in D and I respectively. Yellow arrows in A and F represent the apical localization of PIN1:GFP in epidermis. Arrowheads in H and I represent the termination of the LLD in *unh-1* secondary veins. Areas of high PIN1:GFP expression within marginal cells are flanked by asterisks. Viewed by confocal microscopy. Scale Bars A,B,C,E,F,G,H,J = 10 μM and D,I = 50 μM.

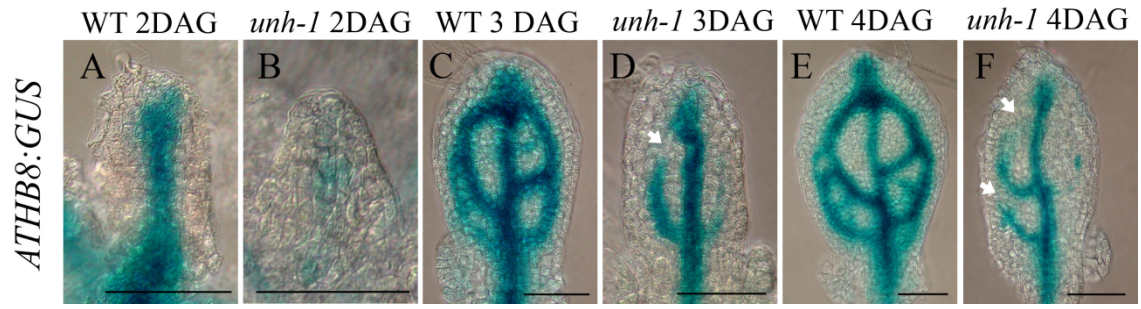

Figure 3.11: *ATHB8:GUS* expression in developing first leaves of wild type (A, C, E) and *unh-1* (B, D, F) seedlings at 2DAG (A-B), 3DAG (C-D), 4DAG (E-F). Arrows in D and F indicate absence of *ATHB8:GUS* expression at distal junctions. Stained for 18 hours, viewed with differential interference contrast. Scale bar = 50 μm.

CHAPTER 4: DISCUSSION

4.1 UNH is a member of the plant GARP complex

I report the identification and characterization of a novel *Arabidopsis* gene, *UNHINGED (UNH)*, which encodes a homologue of the yeast VPS51, the fourth subunit of the tetrameric GARP tethering complex. Previous genomic analyses show high conservation of the VPS51 domain within eukaryotes (Luo et al., 2011). My sequence similarity analysis (Figure 3.5) reveals that UNH/VPS51 shares closest homology to *Oryza sativa* and close similarity to *Physcomitrella patens* and *Chlorella variabilis*, as well as with humans and *Caenorhabditis elegans* (Figure 3.5), indicating an evolutionary conservation of this domain.

Of the three genes present in *Arabidopsis,* only UNH/VPS51 contains an intact LVYENYNKFISATDT motif identified as being highly conserved within multicellular eukaryotes (Luo et al., 2011). My yeast two-hybrid assay shows that UNH/VPS51 interacts with VPS52 (Figure 3.6). Taken together, these results indicate that UNH is a member of the *Arabidopsis* GARP complex. UNH failed to interact with VPS53 and VPS54, the other two subunits of the complex. This is similar to the situation in humans, where ANG2 (VPS 51) shows strong interaction with VPS52 and only weak interaction with VPS53 and VPS54 (Pérez-Victoria et al., 2010b). Similarly, split-YFP experiment done for three components of the *Arabidopsis* GARP complex showed that VPS53 interacts with VPS52 and VPS54 but VPS52 and VPS54 do not interact with each other despite their colocalization at the TGN (Guermonprez et al., 2008; Wang et al., 2011). In contrast, in yeast and *C. elegans,* all the members of the

complex interact with each other (Conibear et al., 2003; Luo et al., 2011; Reggiori et al., 2003; Siniossoglou and Pelham, 2002).

Whereas *unh-1* mutants show a pleiotropic phenotype, the recovery of plants homozygous for either *unh-1* or *unh-2* suggest that these mutations to VPS51 cause neither gametophytic defects nor embryonic lethality. One explanation is that both alleles retain partial function since both mutations are 3' to the region corresponding to the conserved VPS51 domain of UNH (Figure 3.4D-3.4E). A second possibility is that the two other VPS51 domain containing proteins encoded by the *Arabidopsis* genes act in a partially redundant manner, and that their function allows GARP to function in the absence of UNH. A third possibility is that, as in yeast, mammals and *C. elegans*, the VPS51 subunit plays an auxiliary role within the GARP complex. In yeast, whereas loss of VPS52, VPS53 or VPS54 reduces the stability of the other GARP components, loss of VPS51 does not affect their abundance (Conibear et al., 2003). The tethering function of mammalian GARP complex is maintained even in the absence of VPS51 (Perez-Victoria and Bonifacino, 2009; Pérez-Victoria et al., 2008) and in *C. elegans*, loss of the gene encoding VPS51 leads to less reduced brood size compared to mutations in genes encoding the other three components (Luo et al., 2011).

4.2 Ectopic PIN leads to the *unh* phenotype

Mutation to *UNH* results in changes to root growth, leaf epidermal cell undulation, leaf vein pattern and leaf serrations, all characteristics directly mediated by PIN cellular localization. I show that mutation to *PIN1* suppresses the *unh* leaf

epidermal cell, vein pattern and serration phenotypes, whilst mutation to *PIN2* suppresses the *unh* root growth phenotype, suggesting that the spectrum of phenotypes may be explained by over-expression of PIN proteins.

Leaves of *unh-1* have non-meeting secondary veins and form extra serrations, two characteristics that are proposed to be controlled by PIN1 convergence points on the leaf margin (Bilsborough et al., 2011; Rolland-Lagan and Prusinkiewicz, 2005; Scarpella et al., 2006; Wabnik et al., 2010; Wenzel et al., 2007). Plants mutant for *YABBY, VAM3 or ASYMMETRIC LEAF1* (*AS1*) are defective in leaf vein patterning and have ectopic and extended PEDs within the epidermal cells of the leaf margins (Hay et al., 2006; Ohtomo et al., 2005; Sarojam et al., 2010; Shirakawa et al., 2009). In *unh-1* while the sub cellular localization of PIN1:GFP in margin cells appears normal, each marginal PED associated with newly forming secondary veins is expanded. Subsequently, within the secondary vein PED, the formation of the LLD appears normal, but the ULD does not form and no cells with apical or bipolar PIN1 localization are seen (Figure 3.10).

The simplest explanation for the *unh* leaf phenotype is that ectopic PIN1 in the margin leads to higher levels of auxin at the marginal convergence points and alterations to vein patterning and serration development. In addition, *unh-1* may result in ectopic PIN within developing veins at a level too subtle to be detected by my analyses, but sufficient to increase auxin flux within developing veins. Suppression of the *unh-1* vein and serration phenotype by *pin1-1* and partial suppression by *aux1-7* support these proposals. AUX1 is proposed to work together with PIN1 to establish the marginal convergence point: it is localized to the lateral

side of marginal cells allowing retrieval of auxin into the epidermis from subepidermal cells (Bainbridge et al., 2008; Bayer et al., 2009; Reinhardt et al., 2003). Thus, absence of AUX1 is predicted to reduce the auxin levels in the margin and suppress the effects of ectopic PIN1 expression. Whereas localization of AUX1 within developing veins has not been shown, inclusion of an auxin influx activity that increases auxin flux within developing veins provide more accurate models of auxin canalization and vein pattern formation (Kramer, 2009; Wabnik et al., 2010). According to these models, absence of AUX1 in developing veins would reduce the higher auxin flux induced by ectopic PIN1 expression.

Like the interspersed PIN1 convergence points on the leaf margin that define secondary vein and serration position (Bilsborough et al., 2011), interspersed areas of differential PIN localization on the membrane of interdigitated epidermal cells is proposed to define the position of cellular lobes (Li et al., 2011; Xu et al., 2010). Lobes and indentations of interdigitated epidermal cells are thought to result from differential accumulation of hypo-phosphorylated PIN1 in lobes and hyper-phosphorylated PIN1 in indentations (Li et al., 2011). Plants constitutively expressing PIN1 have increased epidermal cell lobing, whereas those constitutively expressing the kinase PINOID, which is responsible for phosphorylating PIN1, have decreased lobing. *unh-1* epidermal cells are more undulated, due to more extensive lobe formation. Evidence that the increased lobes in *unh-1* are the result of ectopic PIN1 is its suppression by the *pin1* mutation. The increased lobes in *unh-1* could be due to increased domains of hypo-phosphorylated PIN1, suggesting a role for the

GARP complex in establishing appropriate domains of PIN1 within the epidermal cells.

The *unh* root is shorter than wild type, possibly due to increased auxin levels within the elongation zone. The *PIN2* allele *eir1-1* suppresses the *unh-1* root phenotype, suggesting that the short root of *unh-1* mutants results from ectopic PIN2, although I was unable to detect differences in PIN2:GFP levels in *unh-1* roots by confocal microscopy. Increased PIN2 in the root epidermis would increase upward auxin flux, resulting in increased auxin levels within the elongation zone. As well, increased PIN2 could increase auxin flux through the root tip, reducing auxin levels within the root tip. The reduction of auxin in the root tip in *unh-1* is consistent with the reduced DR5:GUS expression (Cormark, 2006). Taken together, I conclude that the *unh-1* phenotype is the result of ectopic PIN in various cell types and tissues, and I suggest a role for the GARP complex in the regulation of PIN levels in several developmental processes.

4.3 UNH control of PIN1 expression is mediated by PIN1 vacuolar trafficking

The first observable defect in *unh-1* leaves is larger domains of PIN1 expression at the lateral convergence points of the leaf margin. During development of the wild type leaf, distal convergence points disappear and new, more proximal convergence points emerge due to shifting PIN1 expression and localization (Bilsborough et al., 2011; Scarpella et al., 2006). Emergence of each new convergence point involves a shift in PIN1 expression from apical to basal in cells distal to the new convergence point and a reduction in PIN1 levels in cells above the convergence

point. In *unh-1,* the shift in PIN1 localization within the margin seems to occur normally, but the reduction in PIN1 levels fails to occur completely, resulting in an expanded marginal PED. While the apical to basal shift is believed to be controlled by *CUPSHAPED COTYLEDON2 (CUC2)* (Bilsborough et al., 2011; Kawamura et al., 2010), the mechanism controlling PIN protein abundance within the marginal cells is unknown but likely involves reduced levels of protein synthesis and/or reduced recycling and increased degradation of endocytosed protein**.** The balance between degradation and recycling has been shown to be important in the regulation of root growth (Abas et al., 2006; Kleine-Vehn et al., 2008; Marhavý et al., 2011). Considering the conserved role throughout eukaryotes for the GARP complex in targeting proteins for degradation, I propose that UNH is important for PIN1 degradation. The expanded PED in *unh* would then result from persistent PIN1 in the cells where PIN1 would normally be targeted for degradation.

My finding that UNH interacts with VPS52 (POK) and previous findings that POK::GFP co-localizes with the ST:DsRed, a TGN marker (Lobstein et al., 2004), indicates that UNH and the GARP complex is localized at the TGN in plants. When I investigated the subcellular localization of UNH in tobacco epidermal cells it colocalized with SYP61:YFP domain (Figure 3.7). SYP61, like the yeast TLG1 or mammalian SYP6 is localized to TGN and PVC (Bassham et al., 2000; Sanderfoot et al., 2001). This provides further evidence that UNH/VPS51, a subunit of the GARP complex is localized at the TGN.

Targeting to the vacuole requires the recognition of vesicle cargo by vacuolar sorting receptors (VSRs). The GARP complex in yeast, humans and *C. elegans*

functions in tethering of the late endosome derived VSR at the TGN allowing their utilization in subsequent recognition cycles and maintenance of lysosomal function (Conibear and Stevens, 2000; Luo et al., 2011; Pérez-Victoria et al., 2010b). Previous studies have found three VSR homologous VSR3, VSR4 and VSR7 of the seven VSR homoloues (VSR1-VSR7) identified in *Arabidopsis*, involve SYP61 during vesicle trafficking between PVC and TGN (Drakakaki et al., 2012; Zouhar et al., 2010). I propose that the *Arabidopsis* GARP complex performs a similar role and is required for retrieval of the VSRs at the TGN.

GARP mutation in yeast impairs the recycling of secretory vesicle V-SNARE, Suppressor of the Null allele of CAP (SNC1) and carboxypeptidase Y (CPY) receptor to TGN (Conibear et al., 2003; Reggiori et al., 2003). Similarly, mutation in mammalian GARP complex blocks the recycling of Cation Independent Mannose-6 Phosphate receptor (CIMPR) from the endosome to the TGN leading to missorting of the CIMPR cargo, lysosomal hydrolases, into extracellular space (Pérez-Victoria et al., 2008). I propose that in *unh* mutants, PIN1 proteins fail to be targeted properly to the lytic vacuole within leaf margin cells. Instead, endocytosed PIN1 is recycled back to the PM leading to an expanded lateral PED. Vein pattern defects have previously been associated with defects to vacuolar targeting. Failure to transport PIN1 to the lytic vacuole in *charged multivesicular body protein/chromatin modifying protein1a (chmp1a)* and *chmp1b* mutants leads to ectopic expression of PIN1 proteins and developmental defects including a disorganized and non-meeting cotyledon vein pattern (Spitzer et al., 2009). As well, mutation to the PVC and vacuole localized cognate SNAREs *VTI11* and *VAM3* result in failure to target PIN1:GFP to the vacuole,

expanded marginal PEDs and leaf vein defects very similar to *unh* (Shirakawa et al., 2009). I found that double mutants of *unh-1 vam3* or *unh-1 vti11* resulted in a leaf vein pattern additive between the two single mutants, supporting the idea that they act in independent but partially redundant steps.

4.4 Strength of auxin sources determines vein phenotypes

The enlarged marginal PEDs in *unh-1* are correlated with the lack of distal vein meeting and reduced tertiary and quaternary vein formation (Figure 4.1). I propose that the expanded PED results in a higher marginal auxin source that leads to increased auxin flux through the LLD (compare LLD in Figures 4.1B and 4.1E). Based on the *unh-1* phenotype, I suggest that increased flux in the LLD has two consequences; firstly it drains the auxin within the lamina thereby depleting the auxin required to initiate tertiary and quaternary veins. Secondly, the increased flux alters the relationship between the midvein and secondary vein resulting in an inability to establish a connection between them (compare figures 4.1C and 4.1F). I propose that the auxin sources at the distal tip and lateral convergence points compete in much the same way as the SAM competes with a lateral meristem during lateral bud outgrowth (Prusinkiewicz et al., 2009). According to this model, the relative level of flux through the main stem and the lateral stem compete for ability to localize PIN and transport auxin. If the existing auxin flux from the shoot apical meristem is high, flux from a lateral meristem is prevented (Balla et al 2011). Various processes, such as decapitation or flowering, can alter flux from the apex, allowing flux from lateral buds and lateral outgrowth (Prusinkiewicz et al., 2009). I

propose that flux from the distal leaf tip through the midveins is analogous to flux from the apical meristem, whilst flux from the lateral convergence points through the secondary veins is analogous to flux from the lateral buds. Because the sources of auxin for these fluxes, the margin convergence points, are shifting and reforming more distally throughout leaf development, it seems likely that auxin flux through midveins and consecutive secondary veins is changing over time. In much the same way as flowering reduces auxin flux from the apical meristems and allows flux from lateral buds (Prusinkiewicz et al., 2009), I propose that reducing flux in successive secondary veins through dispersal of the marginal auxin source is critical to allowing auxin flux through the ULD. In *unh-1* mutants, the marginal source is expanded, auxin flux is higher and the ULD fails to form. Interestingly, *forked1 (fkd1)* mutants, which are expected to have reduced auxin flux in secondary veins due to delayed PIN canalization, also fail to form a ULD (Hou et al., 2010). Thus, similar to bud activation where either more (*more axillary branching* (*max*) mutants)) or less (*Toll/IL-1 receptor/plant disease resistance gene* (*tir1*) mutants)) auxin flux from the apex results in increased auxin transport from buds and bud outgrowth (Prusinkiewicz et al., 2009), it seems that either too much or too little flux can inhibit auxin transport through the ULD.

My model for leaf vein patterning highlights the critical importance of marginal convergence points to final vein pattern. The auxin convergence points are also important for the development of serrations, because they establish auxin maxima that drive localized cell division (Bilsborough et al., 2011). Here, I show that *UNH*, acting as part of the GARP complex likely to properly target PIN1 to the lytic

vacuole, is important in establishing the outer boundaries of the convergence point and hence its extent.

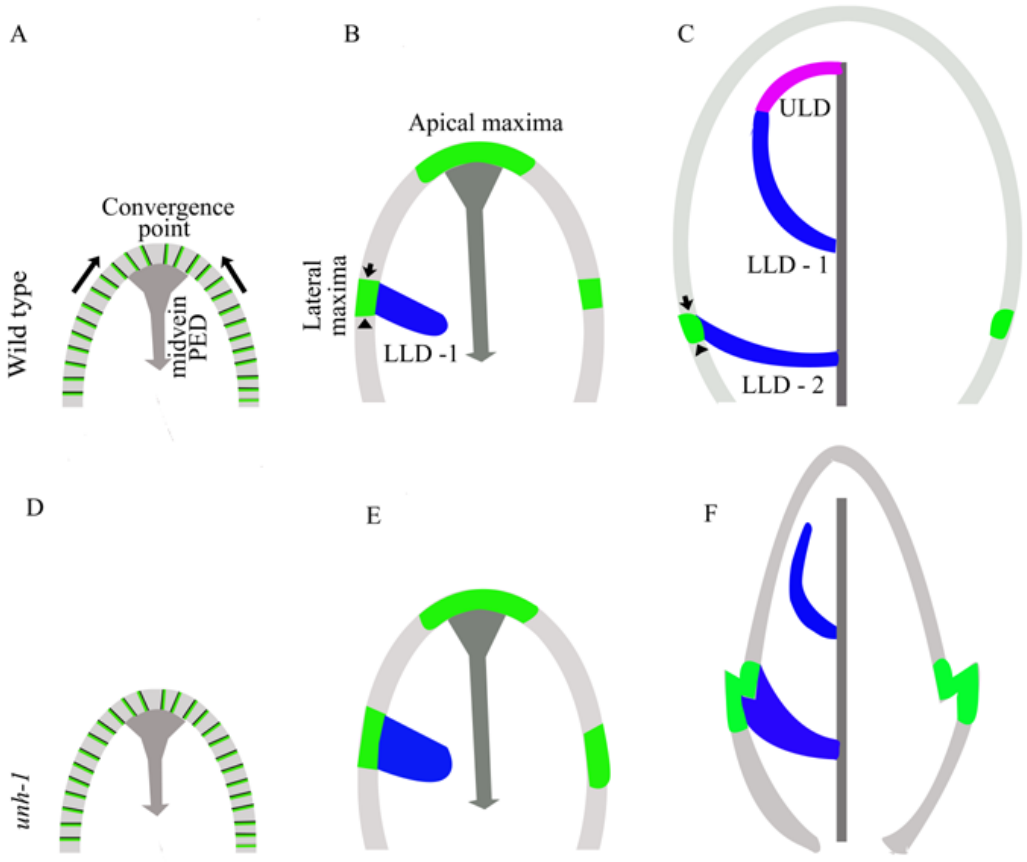

Figure 4.1: Model for UNH function during leaf vein patterning.
(A) and (D) At early stages of WT (A) and *unh* (D) PIN1 is localized apically (green) on all epidermal cells generating a convergence point towards the apex (arrows in A). (B) and (E) The convergence point gives rise to an auxin maximum which generates the midvein PED that is wide distally and narrows proximally. Lateral margin maxima are positioned on the margin due to polarity switch in cells distal to the new maxima (arrow above lateral maxima) and generation of new PED (arrowhead below lateral maxima). The grey regions distal to the maxima along the leaf margin denotes the region where apically localized PIN1:GFP (A and D) is degraded. The lateral maxima initiate LLD - 1 of the first set of secondary veins (blue in B and E). (C) and (F) At subsequent stages in wild type (C) LLD-1 is extended and the PED is completed (C) distally by the ULD (magenta). To generate the second set of secondary veins, the lateral maxima shifts proximally and LLD -2 is initiated. In *unh*, degradation of apically localized PIN:GFP is incomplete, resulting in an extended lateral marginal PED (E). This results in stronger auxin maxima and stronger flux through the LLD relative to the midvein. The flux imbalance leads to an inability to initiate auxin flux through the ULD (E). The length of green for lateral maxima denotes the strength of the maxima and width of LLD (blue) represents the strength of auxin flux in LLD.

CHAPTER 5: CONCLUSIONS

In this work, I used a positional cloning approach to identify and characterize a novel *Arabidopsis* gene, *UNHINGED (UNH)*. *UNH* encodes the *Arabidopsis* homologue of VPS51, the fourth subunit of the plant GARP complex. The GARP complex, previously characterized in yeast and mammals, is a tetrameric tethering complex localized at the Trans-Golgi Network (TGN) and is critical to retrograde transport of Vacuolar Sorting Receptors (VSRs) to the TGN from the late endosomes. The cycling of VSRs determines the efficiency of protein degradation. Mutations in genes encoding the subunits of the GARP complex in yeast, mammals and *C. elegans* show lack of VSR retrieval to the TGN leading to mistargeting of lysosomal proteins and defects to lysosome structure.

I used a yeast 2-hybrid based interaction assay to show that UNH interacts with *Arabidopsis* VPS52, another member of the GARP complex, and hence is a member of the plant GARP complex. The subcellular localization of UNH (VPS51) was investigated by co-expressing 35S:GFP:UNH with 35S:SYP61:YFP, a TGN marker, in tobacco epidermal cells. SYP61 is an *Arabidopsis* homologue of the t-SNARE, TLG1. The colocalization of 35S:GFP:UNH with 35S:YP61:YFP suggested that UNH interacts with SYP61 and is localized at the TGN. This is also consistent with the previous studies in other metozoans, which show that VPS51 interacts with TLG1 and its homologues. Interaction of GARP complex with t-SNAREs is critical for vesicle cycling to regulate the endocytosis and degradation of plasma membrane proteins. My analyses of the phenotypic effects of UNH mutation also suggest that alteration to

the functioning of the GARP complex affects maintenance of PIN levels at the plasma membrane.

Plants mutant for *UNH* show pleiotropic defects associated with auxin regulated development including simpler and non-meeting vein phenotype, more undulated pavement cells in the abaxial epidermis, increased number of serrations in the margins of the first leaf and reduced growth of the shoot and and primary root. These defects are consistent with defects to auxin transport. My results further show that the *unh*-1 phenotype is suppressed in *pin* mutant background suggesting that *unh*-1 phenotype could result from PIN over-expression. To test this idea I compared the PIN1:GFP expression in the first leaves of *unh*-1 with that of wild type and found that in *unh*-1 PIN1:GFP expression is expanded in the regions of lateral auxin maxima that are crucial for secondary vein formation and serrations. On the basis of the role of the GARP complex in other metazoans, I suggest that the expanded expression of PIN1:GFP at the leaf margins is likely due to failure of PIN proteins to be properly targeted to the vacuole. My findings suggest that UNH and therefore the GARP complex in *Arabdiospis* has a role in maintaining PIN1 levels at the plasma membrane possibly through regulating vacuolar targeting of the PIN proteins.

In *Arabidopsis* the localization and interactions amongst three other subunits of the complex VPS52, VPS53 and VPS54 have previously been elucidated. Mutations in the genes encoding these subunits show male transmission defects during fertilization and are homozygous lethal. Thus, analysis of the effect of loss-of-function mutation in these genes during post-embryonic development has not been

possible. In contrast, *unh*-1 and *unh*-2 mutations are viable and show no detectable changes in reproductive organs or their function. This unique feature of *unh*-1 mutations provide an opportunity to study the function of the *Arabidopsis* GARP complex through plant development. The pleiotropic developmental defects resulting from *unh*-1 mutation indicate an important role of the GARP complex in plant development.

Characterization of *UNH* provides insights into a novel mechanism by which the GARP complex affects PIN1 dynamics and reveals a role for the GARP complex in leaf vein patterning process as well as other auxin regulated developmental processes. Since veins in particular are crucial components of plant structure and function, understanding how the vein pattern is regulated will be instrumental for the researchers working in the field of ecology, physiology and evolution.

REFERENCES

Abas, L., Benjamins, R., Malenica, N., Paciorek, T., Wisniewska, J., Moulinier-Anzola, J. C., Sieberer, T., Friml, J. and Luschnig, C. (2006). Intracellular trafficking and proteolysis of the Arabidopsis auxin-efflux facilitator PIN2 are involved in root gravitropism. *Nat. Cell Biol.* **8**, 249-256.

Amberg, D. C., Burke, D. J. and Strathern, J. N. (2005). Methods in yeast genetics: a Cold Spring Harbor laboratory manual. Cold Spring Harbor, New York: Cold Spring Harbor Laboratory Press.

Avsian-Kretchmer, O., Cheng, J. C., Chen, L., Moctezuma, E. and Sung, Z. R. (2002). Indole acetic acid distribution coincides with vascular differentiation pattern during Arabidopsis leaf ontogeny. *Plant Physiol.* **130**, 199-209.

Baima, S., Nobili, F., Sessa, G., Lucchetti, S., Ruberti, I. and Morelli, G. (1995). The expression of the Athb-8 homeobox gene is restricted to provascular cells in Arabidopsis thaliana. *Development* **121**, 4171-4182.

Bainbridge, K., Guyomarc'h, S., Bayer, E., Swarup, R., Bennett, M., Mandel, T. and Kuhlemeier, C. (2008). Auxin influx carriers stabilize phyllotactic patterning. *Genes Dev.* **22**, 810-823.

Bandyopadhyay, A., Blakeslee, J. J., Lee, O. R., Mravec, J., Sauer, M., Titapiwatanakun, B., Makam, S. N., Bouchard, R., Geisler, M., Martinoia, E. et al. (2007). Interactions of PIN and PGP auxin transport mechanisms. *Biochem. Soc. Trans.* **35**, 137-141.

BarPeled, M., Bassham, D. C. and Raikhel, N. V. (1996). Transport of proteins in eukaryotic cells: More questions ahead. *Plant Mol. Biol.* **32**, 223-249.

Bartel, B. (1997). Auxin Biosynthesis. *Annu. Rev. Plant Physiol. Plant Mol. Biol.* **48**, 51-66.

Bartel, P., Chien, C. T., Sternglanz, R. and Fields, S. (1993). Elimination of false positives that arise in using the two-hybrid system. *Biotechniques* **14**, 920-924.

Bassham, D. C., Sanderfoot, A. A., Kovaleva, V., Zheng, H. Y. and Raikhel, N. V. (2000). AtVPS45 complex formation at the trans-Golgi network. *Mol. Biol. Cell* **11**, 2251-2265.

Bayer, E. M., Smith, R. S., Mandel, T., Nakayama, N., Sauer, M., Prusinkiewicz, P. and Kuhlemeier, C. (2009). Integration of transport-based models for phyllotaxis and midvein formation. *Genes Dev.* **23**, 373-384.

Benkova, E., Michniewicz, M., Sauer, M., Teichmann, T., Seifertova, D., Jurgens, G. and Friml, J. (2003). Local, efflux-dependent auxin gradients as a common module for plant organ formation. *Cell* **115**, 591-602.

Bennett, M. J., Marchant, A., Green, H. G., May, S. T., Ward, S. P., Millner, P. A., Walker, A. R., Schulz, B. and Feldmann, K. A. (1996). Arabidopsis AUX1 gene: a permease-like regulator of root gravitropism. *Science* **273**, 948-950.

Bennett, S. R. M., Alvarez, J., Bossinger, G. and Smyth, D. R. (1995). Morphogenesis in Pinoid Mutants of Arabidopsis-Thaliana. *Plant J.* **8**, 505-520.

Berleth, T. and Jurgens, G. (1993). The role of the MONOPTEROS gene in organizing the basal body region of the Arabidopsis embryo. *Development* **118**, 575-587.

Berleth, T. and Mattsson, J. (2000). Vascular development: tracing signals along veins. *Curr. Opin. Plant Biol.* **3**, 406-411.

Berleth, T., Mattsson, J. and Hardtke, C. S. (2000). Vascular continuity and auxin signals. *Trends Plant Sci.* **5**, 387-393.

Besterman, J. M. and Low, R. B. (1983). Endocytosis - a review of mechanisms and plasma-membrane dynamics. *Biochem. J.* **210**, 1-13.

Bilsborough, G. D., Runions, A., Barkoulas, M., Jenkins, H. W., Hasson, A., Galinha, C., Laufs, P., Hay, A., Prusinkiewicz, P. and Tsiantis, M. (2011). Model for the regulation of Arabidopsis thaliana leaf margin development. *Proc. Natl. Acad. Sci. USA* **108**, 3424-3429.

Blackshaw, M.T. (2008). *Molecular characterization of FORKED1 and unhinged.* B.Sc. University of Lethbridge, Canada.

Blakeslee, J. J., Bandyopadhyay, A., Lee, O. R., Mravec, J., Titapiwatanakun, B., Sauer, M., Makam, S. N., Cheng, Y., Bouchard, R., Adamec, J. et al. (2007). Interactions among PIN-FORMED and P-glycoprotein auxin transporters in Arabidopsis. *Plant Cell* **19**, 131-147.

Blilou, I., Xu, J., Wildwater, M., Willemsen, V., Paponov, I., Friml, J., Heidstra, R., Aida, M., Palme, K. and Scheres, B. (2005). The PIN auxin efflux facilitator network controls growth and patterning in Arabidopsis roots. *Nature* **433**, 39-44.

Bonifacino, J. S. and Glick, B. S. (2004). The mechanisms of vesicle budding and fusion. *Cell* **116**, 153-166.

Bonifacino, J. S. and Rojas, R. (2006). Retrograde transport from endosomes to the trans-Golgi network. *Nat. Rev. Mol. Cell Biol.* **7**, 568-579.

Bowers, K. and Stevens, T. H. (2005). Protein transport from the late Golgi to the vacuole in the yeast Saccharomyces cerevisiae. *BBA Mol. Cell. Res.* **1744**, 438-454.

Brandizzi, F., Snapp, E. L., Roberts, A. G., Lippincott-Schwartz, J. and Hawes, C. (2002). Membrane protein transport between the endoplasmic reticulum and the Golgi in tobacco leaves is energy dependent but cytoskeleton independent: evidence from selective photobleaching. *Plant Cell* **14**, 1293-1309.

Braulke, T. and Bonifacino, J. S. (2009). Sorting of lysosomal proteins. *BBA Mol. Cell. Res.* **1793**, 605-614.

Brodsky, F. M., Chen, C. Y., Knuehl, C., Towler, M. C. and Wakeham, D. E. (2001). Biological basket weaving: Formation and function of clathrin-coated vesicles. *Annu. Rev. Cell Dev. Biol.* **17**, 517-568.

Bryant, N. J. and James, D. E. (2001). Vps45p stabilizes the syntaxin homologue Tlg2p and positively regulates SNARE complex formation. *EMBO J.* **20**, 3380-3388.

Burgoyne, R. D. (1990). Secretory vesicle-associated proteins and their role in exocytosis. *Annu. Rev. Physiol.* **52**, 647-659.

Cacan, R. and Verbert, A. (2000). Transport of free and N-linked oligomannoside species across the rough endoplasmic reticulum membranes. *Glycobiology* **10**, 645-648.

Cai, H. Q., Reinisch, K. and Ferro-Novick, S. (2007). Coats, tethers, Rabs, and SNAREs work together to mediate the intracellular destination of a transport vesicle. *Dev. Cell* **12**, 671-682.

Chen, R. J., Hilson, P., Sedbrook, J., Rosen, E., Caspar, T. and Masson, P. H. (1998). The Arabidopsis thaliana AGRAVITROPIC 1 gene encodes a component of the polar-auxin-transport efflux carrier. *Proc. Natl. Acad. Sci. USA* **95**, 15112-15117.

Chen, Y. A. and Scheller, R. H. (2001). SNARE-mediated membrane fusion. *Nat. Rev. Mol. Cell Biol.* **2**, 98-106.

Christensen, S. K., Dagenais, N., Chory, J. and Weigel, D. (2000). Regulation of auxin response by the protein kinase PINOID. *Cell* **100**, 469-478.

Cohen, J. D. and Bandurski, R. S. (1982). Chemistry and physiology of the bound auxins. *Annu. Rev. Plant Physiol. Plant Mol. Biol.* **33**, 403-430.

Conibear, E., Cleck, J. N. and Stevens, T. H. (2003). Vps51p mediates the association of the GARP (Vps52/53/54) complex with the late Golgi t-SNARE Tlg1p. *Mol. Biol. Cell* **14**, 1610-1623.

Conibear, E. and Stevens, T. H. (2000). Vps52p, Vps53p, and Vps54p form a novel multisubunit complex required for protein sorting at the yeast late golgi. *Mol. Biol. Cell* **11**, 305-323.

Cormark, R.D. (2006). *The UNHINGED gene is essential for vascular complexity in the leaves and cotyledons of Arabidopsis.* M.Sc. University of Lethbridge, Canada.

Darwin, C. and Darwin, F. (1880). *The Power of Movement in Plants*. Appleton and Company, New York.

Dellaporta, S.L., Wood, J. and Hicks, J.B. (1983). A plant DNA minipreparation: Version II. *Plant Mol. Biol. Rep.,* **1**, 19-21.

Dettmer, J., Hong-Hermesdorf, A., Stierhof, Y. D. and Schumacher, K. (2006). Vacuolar H+-ATPase activity is required for endocytic and secretory trafficking in Arabidopsis. *Plant Cell* **18**, 715-730.

Dharmasiri, N., Dharmasiri, S. and Estelle, M. (2005). The F-box protein TIR1 is an auxin receptor. *Nature* **435**, 441-445.

Dhonukshe, P., Aniento, F., Hwang, I., Robinson, D. G., Mravec, J., Stierhof, Y. D. and Friml, J. (2007). Clathrin-mediated constitutive endocytosis of PIN auxin efflux carriers in Arabidopsis. *Curr. Biol.* **17**, 520-527.

Drakakaki, G., van de Ven, W., Pan, S. Q., Miao, Y. S., Wang, J. Q., Keinath, N. F., Weatherly, B., Jiang, L. W., Schumacher, K., Hicks, G. et al. (2012). Isolation and proteomic analysis of the SYP61 compartment reveal its role in exocytic trafficking in Arabidopsis. *Cell Res.* **22**, 413-424.

Feraru, E. and Friml, J. (2008). PIN polar targeting. *Plant Physiology* **147**, 1553-1559.

Feraru, E., Paciorek, T., Feraru, M. I., Zwiewka, M., De Groodt, R., De Rycke, R., Kleine-Vehn, J. r. and Friml, J. Ã. (2010). The AP-3 Adaptin mediates the biogenesis and function of lytic vacuoles in Arabidopsis. *Plant Cell* **22**, 2812-2824.

Fluck, R. A., Leber, P. A., Lieser, J. D., Szczerbicki, S. K., Varnes, J. G., Vitale, M. A. and Wolfe, E. E. (2000). Choline conjugates of auxins. I. Direct evidence for the hydrolysis of choline-auxin conjugates by pea cholinesterase. *Plant Physiol. Biochem.* **38**, 301-308.

Friml, J. (2003). Auxin transport - shaping the plant. *Curr Opin Plant Biol* **6**, 7-12.

Friml, J. and Palme, K. (2002). Polar auxin transport--old questions and new concepts? *Plant Mol. Biol.* **49**, 273-284.

Friml, J., Vieten, A., Sauer, M., Weijers, D., Schwarz, H., Hamann, T., Offringa, R. and Jurgens, G. (2003). Efflux-dependent auxin gradients establish the apical-basal axis of Arabidopsis. *Nature* **426**, 147-153.

Friml, J., Wisniewska, J., Benkova, E., Mendgen, K. and Palme, K. (2002). Lateral relocation of auxin efflux regulator PIN3 mediates tropism in Arabidopsis. *Nature* **415**, 806-809.

Friml, J., Yang, X., Michniewicz, M., Weijers, D., Quint, A., Tietz, O., Benjamins, R., Ouwerkerk, P. B., Ljung, K., Sandberg, G. et al. (2004). A PINOID-dependent binary switch in apical-basal PIN polar targeting directs auxin efflux. *Science* **306**, 862-865.

Galweiler, L., Guan, C. H., Muller, A., Wisman, E., Mendgen, K., Yephremov, A. and Palme, K. (1998). Regulation of polar auxin transport by AtPIN1 in Arabidopsis vascular tissue. *Science* **282**, 2226-2230.

Geldner, N., Anders, N., Wolters, H., Keicher, J., Kornberger, W., Muller, P., Delbarre, A., Ueda, T., Nakano, A. and Jurgens, G. (2003). The Arabidopsis GNOM ARF-GEF mediates endosomal recycling, auxin transport, and auxin-dependent plant growth. *Cell* **112**, 219-230.

Geldner, N., Friml, J., Stierhof, Y. D., Jurgens, G. and Palme, K. (2001). Auxin transport inhibitors block PIN1 cycling and vesicle trafficking. *Nature* **413**, 425-528.

Gietz, R. D. and Woods, R. A. (2002). Transformation of yeast by lithium acetate/single-stranded carrier DNA/polyethylene glycol method. *Methods Enzymol.* **350**, 87-96.

Gu, F., Crump, C. M. and Thomas, G. (2001). Trans-Golgi network sorting. *Cell. Mol. Life Sci.* **58**, 1067-1084.

Guermonprez, H., Smertenko, A., Crosnier, M.-T., Durandet, M., Vrielynck, N., Guerche, P., Hussey, P. J., Satiat-Jeunemaitre, B. and Bonhomme, S. (2008). The POK/AtVPS52 protein localizes to several distinct post-Golgi compartments in sporophytic and gametophytic cells. *J. Exp. Bot.* **59**, 3087-3098.

Hardtke, C. S. and Berleth, T. (1998). The Arabidopsis gene MONOPTEROS encodes a transcription factor mediating embryo axis formation and vascular development. *EMBO J.* **17**, 1405-1411.

Hay, A., Barkoulas, M. and Tsiantis, M. (2006). ASYMMETRIC LEAVES1 and auxin activities converge to repress BREVIPEDICELLUS expression and promote leaf development in Arabidopsis. *Development* **133**, 3955-3961.

Hellens, R. P., Edwards, E. A., Leyland, N. R., Bean, S. and Mullineaux, P. M. (2000). pGreen: a versatile and flexible binary Ti vector for Agrobacterium-mediated plant transformation. *Plant Mol. Biol.* **42**, 819-832.

Hooker, T. S., Lam, P., Zheng, H. and Kunst, L. (2007). A core subunit of the RNA-processing/degrading exosome specifically influences cuticular wax biosynthesis in Arabidopsis. *Plant Cell* **19**, 904-913.

Hou, H., Erickson, J., Meservy, J. and Schultz, E. A. (2010). FORKED1 encodes a PH domain protein that is required for PIN1 localization in developing leaf veins. *Plant J.* **63**, 960-973.

Jaillais, Y., Fobis-Loisy, I., MiËge, C. and Gaude, T. (2008). Evidence for a sorting endosome in Arabidopsis root cells. *Plant J.* **53**, 237-247.

Jaillais, Y., Fobis-Loisy, I., Miege, C., Rollin, C. and Gaude, T. (2006). AtSNX1 defines an endosome for auxin-carrier trafficking in Arabidopsis. *Nature* **443**, 106-109.

Jaillais, Y., Santambrogio, M., Rozier, F., Fobis-Loisy, I., Miege, C. and Gaude, T. (2007). The retromer protein VPS29 links cell polarity and organ initiation in plants. *Cell* **130**, 1057-1070.

Jander, G., Norris, S. R., Rounsley, S. D., Bush, D. F., Levin, I. M. and Last, R. L. (2002). Arabidopsis map-based cloning in the post-genome era. *Plant Physiol.* **129**, 440-450.

Kang, J. and Dengler, N. (2002). Cell cycling frequency and expression of the homeobox gene ATHB-8 during leaf vein development in Arabidopsis. *Planta* **216**, 212-219.

Kato, T., Morita, M. T., Fukaki, H., Yamauchi, Y., Uehara, M., Niihama, M. and Tasaka, M. (2002). SGR2, a phospholipase-like protein, and ZIG/SGR4, a SNARE, are involved in the shoot gravitropism of Arabidopsis. *Plant Cell* **14**, 33-46.

Katzmann, D. J., Babst, M. and Emr, S. D. (2001). Ubiquitin-dependent sorting into the multivesicular body pathway requires the function of a conserved endosomal protein sorting complex, ESCRT-I. *Cell* **106**, 145-155.

Katzmann, D. J., Stefan, C. J., Babst, M. and Emr, S. D. (2003). Vps27 recruits ESCRT machinery to endosomes during MVB sorting. *J. Cell Biol.* **162**, 413-423.

Kawamura, E., Horiguchi, G. and Tsukaya, H. (2010). Mechanisms of leaf tooth formation in Arabidopsis. *Plant J.* **62**, 429-441.

Kleinboelting, N., Huep, G., Kloetgen, A., Viehoever, P. and Weisshaar, B. (2012). GABI-Kat SimpleSearch: new features of the Arabidopsis thaliana T-DNA mutant database. *Nucleic Acids Res.* **40**, D1211-D1215.

Kleine-Vehn, J., Leitner, J., Zwiewka, M., Sauer, M., Abas, L., Luschnig, C. and Friml, J. (2008). Differential degradation of PIN2 auxin efflux carrier by retromer-dependent vacuolar targeting. *Proc. Natl. Acad. Sci. USA* **105**, 17812-17817.

Kohalmi, S. E., Nowak, J. and Crosby, W. L. (1997). A practical guide to using the yeast 2-hybrid system. In *In Differentially expressed genes in plants: a bench manual* (ed. E. a. H. Hansen, G.), pp. 63-82. London: Taylor and Francis.

Kohalmi, S. E., Reader, L. J. V., Samach, A., Nowak, J., Haughn, G. W. and Crosby, W. L. (1998). Identification and characterization of protein interactions using the yeast 2-hybrid system. *Plant Molecular Biology Manual* **M1**, 1-30.

Koumandou, V. L., Dacks, J. B., Coulson, R. M. R. and Field, M. C. (2007). Control systems for membrane fusion in the ancestral eukaryote; evolution of tethering complexes and SM proteins. *Bmc Evolutionary Biology* **7**.

Kramer, E. M. (2009). Auxin-regulated cell polarity: an inside job? *Trends Plant Sci.* **14**, 242-247.

Kramer, E. M. and Bennett, M. J. (2006). Auxin transport: a field in flux. *Trends Plant Sci.* **11**, 382-386.

Last, R. L., Bissinger, P. H., Mahoney, D. J., Radwanski, E. R. and Fink, G. R. (1991). Tryptophan mutants in Arabidopsis - the consequences of duplicated tryptophan synthase beta genes. *Plant Cell* **3**, 345-358.

Laxmi, A., Pan, J., Morsy, M. and Chen, R. (2008). Light plays an essential role in intracellular distribution of auxin efflux carrier PIN2 in Arabidopsis thaliana. *Plos One* **3**, e1510.

Lee, C. F., Pu, H. Y., Wang, L. C., Sayler, R. J., Yeh, C. H. and Wu, S. J. (2006). Mutation in a homolog of yeast Vps53p accounts for the heat and osmotic hypersensitive phenotypes in Arabidopsis hit1-1 mutant. *Planta* **224**, 330-338.

Li, H. J., Lin, D. S., Dhonukshe, P., Nagawa, S., Chen, D. D., Friml, J., Scheres, B., Guo, H. W. and Yang, Z. B. (2011). Phosphorylation switch modulates the interdigitated pattern of PIN1 localization and cell expansion in Arabidopsis leaf epidermis. *Cell Res.* **21**, 970-978.

Li, Y., Hagen, G. and Guilfoyle, T. J. (1991). An Auxin-responsive promoter Is differentially induced by auxin gradients during tropisms. *Plant Cell* **3**, 1167-1175.

Ljung, K., Bhalerao, R. P. and Sandberg, G. (2001). Sites and homeostatic control of auxin biosynthesis in Arabidopsis during vegetative growth. *Plant J.* **28**, 465-474.

Ljung, K., Hull, A. K., Celenza, J., Yamada, M., Estelle, M., Normanly, J. and Sandberg, G. (2005). Sites and regulation of auxin biosynthesis in Arabidopsis roots. *Plant Cell* **17**, 1090-1104.

Ljung, K., Hull, A. K., Kowalczyk, M., Marchant, A., Celenza, J., Cohen, J. D. and Sandberg, G. (2002). Biosynthesis, conjugation, catabolism and homeostasis of indole-3-acetic acid in Arabidopsis thaliana. *Plant Mol. Biol.* **49**, 249-272.

Lobstein, E., Guyon, A., Ferault, M., Twell, D., Pelletier, G. and Bonhomme, S. (2004). The putative Arabidopsis homolog of yeast Vps52p Is required for pollen tube elongation, localizes to golgi, and might be involved in vesicle trafficking. *Plant Physiol.* **135**, 1480-1490.

Luo, L., Hannemann, M., Koenig, S., Hegermann, J., Ailion, M., Cho, M.-K., Sasidharan, N., Zweckstetter, M., Rensing, S. A. and Eimer, S. (2011). The Caenorhabditis elegans GARP complex contains the conserved Vps51 subunit and is required to maintain lysosomal morphology. *Mol. Biol. Cell* **22**, 2564-2578.

Lupashin, V. and Sztul, E. (2005). Golgi tethering factors. *Biochimica Et Biophysica Acta-Molecular Cell Research* **1744**, 325-339.

Luschnig, C., Gaxiola, R. A., Grisafi, P. and Fink, G. R. (1998). EIR1, a root-specific protein involved in auxin transport, is required for gravitropism in Arabidopsis thaliana. *Genes Dev.* **12**, 2175-2187.

Marchant, A., Kargul, J., May, S. T., Muller, P., Delbarre, A., Perrot-Rechenmann, C. and Bennett, M. J. (1999). AUX1 regulates root gravitropism in Arabidopsis by facilitating auxin uptake within root apical tissues. *EMBO J.* **18**, 2066-2073.

Marchler-Bauer, A., Lu, S., Anderson, J. B., Chitsaz, F., Derbyshire, M. K., DeWeese-Scott, C., Fong, J. H., Geer, L. Y., Geer, R. C., Gonzales, N. R. et al. (2011). CDD: a Conserved Domain Database for the functional annotation of proteins. *Nucleic Acids Res.* **39**, D225-D229.

Marcusson, E. G., Horazdovsky, B. F., Cereghino, J. L., Gharakhanian, E. and Emr, S. D. (1994). The sorting receptor for yeast vacuolar carboxypeptidase-Y is encoded by the Vps10 gene. *Cell* **77**, 579-586.

Marhavý, P., Bielach, A., Abas, L., Abuzeineh, A., Duclercq, J., Tanaka, H., PaYezová, M., Petráaek, J., Friml, J., Kleine-Vehn, J. et al. (2011). Cytokinin modulates endocytic trafficking of PIN1 auxin efflux carrier to control plant organogenesis. *Dev. Cell* **21**, 796-804.

Mattsson, J., Sung, Z. R. and Berleth, T. (1999). Responses of plant vascular systems to auxin transport inhibition. *Development* **126**, 2979-2991.

Mayer, U. and Jurgens, G. (1998). Pattern formation in plant embryogenesis: A reassessment. *Semin. Cell Dev. Biol.* **9**, 187-193.

Michniewicz, M., Zago, M. K., Abas, L., Weijers, D., Schweighofer, A., Meskiene, I., Heisler, M. G., Ohno, C., Zhang, J., Huang, F. et al. (2007). Antagonistic regulation of PIN phosphorylation by PP2A and PINOID directs auxin flux. *Cell* **130**, 1044-56.

Minamisawa, N., Sato, M., Cho, K.-H., Ueno, H., Takechi, K., Kajikawa, M., Yamato, K. T., Ohyama, K., Toyooka, K., Kim, G.-T. et al. (2011). ANGUSTIFOLIA, a plant homolog of CtBP/BARS, functions outside the nucleus. *The Plant Journal*, no-no.

Muday, G. K. and DeLong, A. (2001). Polar auxin transport: controlling where and how much. *Trends Plant Sci.* **6**, 535-542.

Muday, G. K., Peer, W. A. and Murphy, A. S. (2003). Vesicular cycling mechanisms that control auxin transport polarity. *Trends Plant Sci.* **8**, 301-304.

Muller, A., Guan, C., Galweiler, L., Tanzler, P., Huijser, P., Marchant, A., Parry, G., Bennett, M., Wisman, E. and Palme, K. (1998). AtPIN2 defines a locus of Arabidopsis for root gravitropism control. *EMBO J.* **17**, 6903-6911.

Niemes, S., Langhans, M., Viotti, C., Scheuring, D., Yan, M. S. W., Jiang, L. W., Hillmer, S., Robinson, D. G. and Pimpl, P. (2010). Retromer recycles vacuolar sorting receptors from the trans-Golgi network. *Plant J.* **61**, 107-121.

Noh, B., Murphy, A. S. and Spalding, E. P. (2001). Multidrug resistance-like genes of Arabidopsis required for auxin transport and auxin-mediated development. *Plant Cell* **13**, 2441-2454.

Normanly, J. and Bartel, B. (1999). Redundancy as a way of life - IAA metabolism. *Curr. Opin. Plant Biol.* **2**, 207-213.

Normanly, J., Cohen, J. D. and Fink, G. R. (1993). Arabidopsis-Thaliana Auxotrophs Reveal a Tryptophan-Independent Biosynthetic-Pathway for Indole-3-Acetic-Acid. *Proc. Natl. Acad. Sci. USA* **90**, 10355-10359.

Ohtomo, I., Ueda, H., Shimada, T., Nishiyama, C., Komoto, Y., Hara-Nishimura, I. and Takahashi, T. (2005). Identification of an allele of VAM3/SYP22 that confers a semi-dwarf phenotype in Arabidopsis thaliana. *Plant Cell Physiol.* **46**, 1358-1365.

Okada, K., Ueda, J., Komaki, M. K., Bell, C. J. and Shimura, Y. (1991). Requirement of the auxin polar transport system in early stages of Arabidopsis floral bud formation. *Plant Cell* **3**, 677-684.

Oliviusson, P., Heinzerling, O., Hillmer, S., Hinz, G., Tse, Y. C., Jiang, L. and Robinson, D. G. (2006). Plant retromer, localized to the prevacuolar compartment and microvesicles in Arabidopsis, may interact with vacuolar sorting receptors. *Plant Cell* **18**, 1239-1252.

Ostin, A., Kowalyczk, M., Bhalerao, R. P. and Sandberg, G. (1998). Metabolism of indole-3-acetic acid in Arabidopsis. *Plant Physiol.* **118**, 285-296.

Paciorek, T., Zazimalova, E., Ruthardt, N., Petrasek, J., Stierhof, Y. D., Kleine-Vehn, J., Morris, D. A., Emans, N., Jurgens, G., Geldner, N. et al. (2005). Auxin inhibits endocytosis and promotes its own efflux from cells. *Nature* **435**, 1251-1256.

Parry, G., Delbarre, A., Marchant, A., Swarup, R., Napier, R., Perrot-Rechenmann, C. and Bennett, M. J. (2001). Novel auxin transport inhibitors phenocopy the auxin influx carrier mutation aux1. *Plant J.* **25**, 399-406.

Peer, W. A., Bandyopadhyay, A., Blakeslee, J. J., Makam, S. I., Chen, R. J., Masson, P. H. and Murphy, A. S. (2004). Variation in expression and protein localization of the PIN family of auxin efflux facilitator proteins in flavonoid mutants with altered auxin transport in Arabidopsis thaliana. *Plant Cell* **16**, 1898-1911.

Pérez-Victoria, F. J., Abascal-Palacios, G., Tascon, I., Kajava, A., Magadan, J. G., Pioro, E. P., Bonifacino, J. S. and Hierro, A. (2010a). Structural basis for the wobbler mouse neurodegenerative disorder caused by mutation in the Vps54 subunit of the GARP complex. *Proc. Natl. Acad. Sci. USA* **107**, 12860-12865.

Perez-Victoria, F. J. and Bonifacino, J. S. (2009). Dual roles of the mammalian GARP complex in Tethering and SNARE complex assembly at the trans-Golgi network. *Mol. Cell. Biol.* **29**, 5251-5263.

Pérez-Victoria, F. J., Mardones, G. A. and Bonifacino, J. S. (2008). Requirement of the human GARP complex for mannose 6-phosphate-receptor-dependent sorting of cathepsin D to lysosomes. *Mol. Biol. Cell* **19**, 2350-2362.

Pérez-Victoria, F. J., Schindler, C., Magadan, J. G., Mardones, G. A., Delevoye, C., Romao, M., Raposo, G. and Bonifacino, J. S. (2010b). Ang2/fat-free is a conserved subunit of the Golgi-associated retrograde protein complex. *Mol. Biol. Cell* **21**, 3386-3395.

Petrasek, J. and Friml, J. (2009). Auxin transport routes in plant development. *Development* **136**, 2675-2688.

Petrasek, J., Mravec, J., Bouchard, R., Blakeslee, J. J., Abas, M., Seifertova, D., Wisniewska, J., Tadele, Z., Kubes, M., Covanova, M. et al. (2006). PIN proteins perform a rate-limiting function in cellular auxin efflux. *Science* **312**, 914-918.

Prusinkiewicz, P., Crawford, S., Smith, R. S., Ljung, K., Bennett, T., Ongaro, V. and Leyser, O. (2009). Control of bud activation by an auxin transport switch. *Proc. Natl. Acad. Sci. USA* **106**, 17431-17436.

Rashotte, A. M., DeLong, A. and Muday, G. K. (2001). Genetic and chemical reductions in protein phosphatase activity alter auxin transport, gravity response, and lateral root growth. *Plant Cell* **13**, 1683-1697.

Reggiori, F., Wang, C.-W., Stromhaug, P. E., Shintani, T. and Klionsky, D. J. (2003). Vps51 Is part of the yeast Vps fifty-three tethering complex essential for retrograde traffic from the early endosome and cvt vesicle completion. *J. Biol. Chem.* **278**, 5009-5020.

Reinhardt, D., Pesce, E. R., Stieger, P., Mandel, T., Baltensperger, K., Bennett, M., Traas, J., Friml, J. and Kuhlemeier, C. (2003). Regulation of phyllotaxis by polar auxin transport. *Nature* **426**, 255-260.

Robinson, D. G., Jiang, L. and Schumacher, K. (2008). The endosomalsystem of plants: charting new and familiar territories. *Plant Physiol.* **147**, 1482-1492.

Robinson, M. S. (1994). The role of clathrin, adapters and dynamin in endocytosis. *Curr. Opin. Cell Biol.* **6**, 538-544.

Rogg, L. E. and Bartel, B. (2001). Auxin signaling: Derepression through regulated proteolysis. *Dev. Cell* **1**, 595-604.

Rolland-Lagan, A. G., Coen, E., Impey, S. J. and Bangham, J. A. (2005). A computational method for inferring growth parameters and shape changes during development based on clonal analysis. *J. Theor. Biol.* **232**, 157-177.

Rolland-Lagan, A. G. and Prusinkiewicz, P. (2005). Reviewing models of auxin canalization in the context of leaf vein pattern formation in Arabidopsis. *Plant J.* **44**, 854-865.

Rubery, P. H. and Sheldrak, A. R. (1974). Carrier-Mediated Auxin Transport. *Planta* **118**, 101-121.

Ruegger, M., Dewey, E., Gray, W. M., Hobbie, L., Turner, J. and Estelle, M. (1998). The TIR1 protein of Arabidopsis functions in auxin response and is related to human SKP2 and yeast grr1p. *Genes Dev.* **12**, 198-207.

Sabatini, S., Beis, D., Wolkenfelt, H., Murfett, J., Guilfoyle, T., Malamy, J., Benfey, P., Leyser, O., Bechtold, N., Weisbeek, P. et al. (1999). An auxin-dependent distal organizer of pattern and polarity in the Arabidopsis root. *Cell* **99**, 463-472.

Sanderfoot, A. A., Assaad, F. F. and Raikhel, N. V. (2000). The Arabidopsis genome. An abundance of soluble N-ethylmaleimide-sensitive factor adaptor protein receptors. *Plant Physiol.* **124**, 1558-1569.

Sanderfoot, A. A., Pilgrim, M., Adam, L. and Raikhel, N. V. (2001). Disruption of individual members of Arabidopsis syntaxin gene families indicates each has essential functions. *Plant Cell* **13**, 659-666.

Sarojam, R., Sappl, P. G., Goldshmidt, A., Efroni, I., Floyd, S. K., Eshed, Y. and Bowman, J. L. (2010). Differentiating Arabidopsis shoots from leaves by combined YABBY activities. *Plant Cell* **22**, 2113-2130.

Scarpella, E., Barkoulas, M. and Tsiantis, M. (2010). Control of leaf and vein development by auxin. *Cold Spring Harb. Perspect Biol.* **2**, a001511.

Scarpella, E., Francis, P. and Berleth, T. (2004). Stage-specific markers define early steps of procambium development in Arabidopsis leaves and correlate termination of vein formation with mesophyll differentiation. *Development* **131**, 3445-3455.

Scarpella, E., Marcos, D., Friml, J. and Berleth, T. (2006). Control of leaf vascular patterning by polar auxin transport. *Genes Dev.* **20**, 1015-1027.

Scheres, B., Wolkenfelt, H., Willemsen, V., Terlouw, M., Lawson, E., Dean, C. and Weisbeek, P. (1994). Embryonic origin of the Arabidopsis primary root and root-meristem Initials. *Development* **120**, 2475-2487.

Schmitt-John, T., Drepper, C., Mussmann, A., Hahn, P., Kuhlmann, M., Thiel, C., Hafner, M., Lengeling, A., Heimann, P., Jones, J. M. et al. (2005). Mutation of Vps54 causes motor neuron disease and defective spermiogenesis in the wobbler mouse. *Nat. Genet.* **37**, 1213-1215.

Seaman, M. N. (2005). Recycle your receptors with retromer. *Trends Cell Biol.* **15**, 68-75.

Seaman, M. N. J., McCaffery, J. M. and Emr, S. D. (1998). A membrane coat complex essential for endosome-to-Golgi retrograde transport in yeast. *J. Cell Biol.* **142**, 665-681.

Shimada, T., Koumoto, Y., Li, L., Yamazaki, M., Kondo, M., Nishimura, M. and Hara-Nishimura, I. (2006). AtVPS29, a putative component of a retromer complex, is required for the efficient sorting of seed storage proteins. *Plant Cell Physiol.* **47**, 1187-1194.

Shin, H., Shin, H. S., Guo, Z. B., Blancaflor, E. B., Masson, P. H. and Chen, R. J. (2005). Complex regulation of Arabidopsis AGR1/PIN2-mediated root gravitropic

response and basipetal auxin transport by cantharidin-sensitive protein phosphatases. *Plant J.* **42**, 188-200.

Shirakawa, M., Ueda, H., Shimada, T., Nishiyama, C. and Hara-Nishimura, I. (2009). Vacuolar SNAREs function in the formation of the leaf vascular network by regulating auxin distribution. *Plant Cell Physiol.* **50**, 1319-1328.

Sieburth, L. E. (1999). Auxin is required for leaf vein pattern in Arabidopsis. *Plant Physiol.* **121**, 1179-1190.

Siniossoglou, S. and Pelham, H. R. (2002). Vps51p links the VFT complex to the SNARE Tlg1p. *J. Biol. Chem.* **277**, 48318-48324.

Siniossoglou, S. and Pelham, H. R. B. (2001). An effector of Ypt6p binds the SNARE Tlg1p and mediates selective fusion of vesicles with late Golgi membranes. *EMBO J.* **20**, 5991-5998.

Sorkin, A. and von Zastrow, M. (2002). Signal transduction and endocytosis: Close encounters of many kinds. *Nat. Rev. Mol. Cell Biol.* **3**, 600-614.

Spitzer, C., Reyes, F. C., Buono, R., Sliwinski, M. K., Haas, T. J. and Otegui, M. S. (2009). The ESCRT-related CHMP1A and B proteins mediate multivesicular body sorting of auxin carriers in Arabidopsis and are required for plant development. *Plant Cell* **21**, 749-766.

Steinmann, T., Geldner, N., Grebe, M., Mangold, S., Jackson, C. L., Paris, S., Galweiler, L., Palme, K. and Jurgens, G. (1999). Coordinated polar localization of auxin efflux carrier PIN1 by GNOM ARF GEF. *Science* **286**, 316-318.

Steynen, Q. J. and Schultz, E. A. (2003). The FORKED genes are essential for distal vein meeting in Arabidopsis. *Development* **130**, 4695-4708.

Surpin, M. and Raikhel, N. (2004). Traffic jams affect plant development and signal transduction. *Nat. Rev. Mol. Cell Biol.* **5**, 329-329.

Swarup, R., Friml, J., Marchant, A., Ljung, K., Sandberg, G., Palme, K. and Bennett, M. (2001). Localization of the auxin permease AUX1 suggests two functionally distinct hormone transport pathways operate in the Arabidopsis root apex. *Genes Dev.* **15**, 2648-2653.

Swarup, R., Kargul, J., Marchant, A., Zadik, D., Rahman, A., Mills, R., Yemm, A., May, S., Williams, L., Millner, P. et al. (2004). Structure-function analysis of the presumptive Arabidopsis auxin permease AUX1. *Plant Cell* **16**, 3069-3083.

Takai, Y., Sasaki, T. and Matozaki, T. (2001). Small GTP-binding proteins. *Physiol. Rev.* **81**, 153-208.

Tam, Y. Y., Epstein, E. and Normanly, J. (2000). Characterization of auxin conjugates in arabidopsis. Low steady-state levels of indole-9-acetyl-aspartate indole-3-acetyl-glutamate, and indole-3-acetyl-glucose. *Plant Physiol.* **123**, 589-595.

Tan, X., Calderon-Villalobos, L. I. A., Sharon, M., Zheng, C. X., Robinson, C. V., Estelle, M. and Zheng, N. (2007). Mechanism of auxin perception by the TIR1 ubiquitin ligase. *Nature* **446**, 640-645.

Tiwari, S. B., Wang, X. J., Hagen, G. and Guilfoyle, T. J. (2001). AUX/IAA proteins are active repressors, and their stability and activity are modulated by auxin. *Plant Cell* **13**, 2809-2822.

Ulmasov, T., Murfett, J., Hagen, G. and Guilfoyle, T. J. (1997). Aux/IAA proteins repress expression of reporter genes containing natural and highly active synthetic auxin response elements. *Plant Cell* **9**, 1963-1971.

Vida, T. A. and Emr, S. D. (1995). A new vital stain for visualizing vacuolar membrane dynamics and endocytosis in yeast. *J. Cell Biol.* **128**, 779-792.

Vieten, A., Sauer, M., Brewer, P. B. and Friml, J. (2007). Molecular and cellular aspects of auxin-transport-mediated development. *Trends Plant Sci.* **12**, 160-168.

Vieten, A., Vanneste, S., Wisniewska, J., Benkova, E., Benjamins, R., Beeckman, T., Luschnig, C. and Friml, J. (2005). Functional redundancy of PIN proteins is accompanied by auxin-dependent cross-regulation of PIN expression. *Development* **132**, 4521-4531.

Viotti, C., Bubeck, J., Stierhof, Y. D., Krebs, M., Langhans, M., van den Berg, W., van Dongen, W., Richter, S., Geldner, N., Takano, J. et al. (2010). Endocytic and secretory traffic in Arabidopsis merge in the trans-Golgi network/early endosome, an independent and highly dynamic organelle. *Plant Cell* **22**, 1344-1357.

Vitale, A. and Hinz, G. (2005). Sorting of proteins to storage vacuoles: how many mechanisms? *Trends Plant Sci.* **10**, 316-323.

Wabnik, K., Kleine-Vehn, J., Balla, J., Sauer, M., Naramoto, S., Reinohl, V., Merks, R. M., Govaerts, W. and Friml, J. (2010). Emergence of tissue polarization from synergy of intracellular and extracellular auxin signaling. *Mol. Syst. Biol.* **6**, 447.

Wang, L. C., Tsai, M. C., Chang, K. Y., Fan, Y. S., Yeh, C. H. and Wu, S. J. (2011). Involvement of the *Arabidopsis* HIT1/AtVPS53 tethering protein homologue in the acclimation of the plasma membrane to heat stress. *J. Exp. Bot.* **62**, 3609-3620.

Went, F.W. and Thimann, K.V. (1937). *Phytohormones*. Macmillan, New York.

Wenzel, C. L., Schuetz, M., Yu, Q. and Mattsson, J. (2007). Dynamics of MONOPTEROS and PIN-FORMED1 expression during leaf vein pattern formation in Arabidopsis thaliana. *Plant J.* **49**, 387-398.

Whyte, J. R. C. and Munro, S. (2002). Vesicle tethering complexes in membrane traffic. *J. Cell Sci.* **115**, 2627-2637.

Wu, S. J., Locy, R. D., Shaw, J. J., Cherry, J. H. and Singh, N. K. (2000). Mutation in Arabidopsis HIT1 locus causing heat and osmotic hypersensitivity. *J. Plant Physiol.* **157**, 543-547.

Xu, T. D., Wen, M. Z., Nagawa, S., Fu, Y., Chen, J. G., Wu, M. J., Perrot-Rechenmann, C., Friml, J., Jones, A. M. and Yang, Z. (2010). Cell surface- and Rho GTPase-based auxin signaling controls cellular interdigitation in Arabidopsis. *Cell* **143**, 99-110.

Yamazaki, M., Shimada, T., Takahashi, H., Tamura, K., Kondo, M., Nishimura, M. and Hara-Nishimura, I. (2008). Arabidopsis VPS35, a retromer component, is required for vacuolar protein sorting and involved in plant growth and leaf senescence. *Plant Cell Physiol.* **49**, 678-678.

Yang, Y. D., Hammes, U. Z., Taylor, C. G., Schachtman, D. P. and Nielsen, E. (2006). High-affinity auxin transport by the AUX1 influx carrier protein. *Curr. Biol.* **16**, 1123-1127.

Zhao, Y. (2010). Auxin biosynthesis and its role in plant development. *Annu. Rev. Plant Biol.* **61**, 49-64.

Zouhar, J., Munoz, A. and Rojo, E. (2010). Functional specialization within the vacuolar sorting receptor family: VSR1, VSR3 and VSR4 sort vacuolar storage cargo in seeds and vegetative tissues. *Plant J.* **64**, 577-588.